JOURNAL OF AIRCRAFT
Vol. 44, No. 1, January–February 2007

Investigation on Conditions of Minimum Induced Drag of Closed Wing Systems and C-Wings

Luciano Demasi*
University of Washington, Seattle, Washington 98195-2400

DOI: 10.2514/1.21884

A theoretical method for predicting minimum induced-drag conditions in a nonplanar lifting systems is presented in this paper. The procedure is based on lifting line theory and the small perturbation acceleration potential. Under the hypotheses of linearity and rigid wake aligned with the freestream, optimality conditions are formulated using the Euler–Lagrange integral equation with constraints on fixed total lifting force and wing span. Particular attention is paid to analysis and numerical treatment of the Hadamard finite-part integrals involved in the solution process. The minimum induced-drag problem is then formulated and solved numerically and analytically. In the case of annular wings, closed-form expressions for the optimal circulation distribution, the normalwash, the induced-drag coefficient, and the efficiency are presented. Optimal annular wings and C-wings are extensively analyzed, and comparisons with available results in the literature are presented. It is confirmed that a C-wing presents almost the same induced drag (under optimal conditions) as the corresponding closed-wing system. However, the optimal distributions of circulation are significantly different. All optimal wing systems are also compared to an optimal cantilevered wing and a biplane.

Nomenclature

a_w	=	semiaxis in the direction of the lift (elliptical annular wing)
C_{D_i}	=	coefficient of induced drag
C_L	=	coefficient of lift
C_1, C_2	=	constants
$\bar{C}$	=	prescribed value of the constraint
$\bar{C}_L$	=	prescribed coefficient of lift (constraint)
c	=	parameter used in the coordinate transformations (elliptical annular wings and arcs)
$c(t)$	=	auxiliary function used in the definition of the constraint
D_i	=	induced drag
E	=	aerodynamic efficiency
F	=	aerodynamic force per unit of length
g_1	=	known symmetric function
g_2	=	known function
H	=	distance between the two wings in a biplane
H_3, H_4	=	auxiliary variables
H_5, H_6, H_7	=	auxiliary variables
$\bar{H}_3$, $\bar{H}_4$	=	auxiliary variables
$\bar{H}_5$, $\bar{H}_6$, $\bar{H}_7$	=	auxiliary variables
I_A, I_B, I_C	=	integrals calculated using a sinusoidal doublet distribution
I'_A, I'_B	=	integrals calculated using a constant doublet distribution
$\boldsymbol{i}$, $\boldsymbol{j}$, $\boldsymbol{k}$	=	unit vectors corresponding to the directions x, y and z
J	=	functional that has to be minimized (induced drag or coefficient of induced drag)
L	=	lift
$\bar{L}$	=	prescribed lift (constraint)
l	=	chord
m	=	doublet distribution
m_{opt}	=	candidate function which minimizes J, optimal doublet distribution
m_0, m_1	=	values of m at the lower and upper limits of the integrals
$\boldsymbol{N}_d$	=	unit vector which acts outward from the local center of curvature
$\boldsymbol{n}_d$	=	unit vector which acts inward from the local center of curvature
q	=	dynamic pressure
R	=	radial coordinate
R_w	=	radius of the circular annular wing
S	=	reference surface
s_d	=	curvilinear coordinate
T_1, T_2, T_3	=	auxiliary variables
$\bar{T}_1$, $\bar{T}_2$, $\bar{T}_3$	=	auxiliary variables
t, s	=	variables used in the computations of the integrals
u_n	=	normalwash
V_∞	=	freestream velocity
X	=	nondimensional x coordinate
x, y, z	=	coordinate system
x_d, y_d, z_d	=	coordinates of the point in which the generic doublet is positioned
$\bar{Y}$	=	symmetric kernel
${}^R\bar{Y}$	=	symmetric regular kernel
${}^S\bar{Y}$	=	symmetric singular kernel (order of the singularity 2)
α	=	twist distribution
α_i	=	induced angle of attack
β	=	angle between the local aerodynamic force and the wing span direction
β_1, β_2	=	lower and upper limits of the integrals (elliptical lifting arcs)
Γ	=	circulation
Δ	=	auxiliary variable
δ	=	variational operator
ε	=	nondimensional parameter used in the geometric definitions of the elliptical lifting arcs
ϑ	=	angle of inclination of the lifting element
λ	=	Lagrange multiplier
ρ_∞	=	density (constant in all field)
σ	=	auxiliary variable used in the derivation of the Euler–Lagrange equation
τ	=	dummy variable

Received 19 December 2005; revision received 31 July 2006; accepted for publication 1 August 2006.

*Post Doctoral Research Associate, Box 352400, Department of Aeronautics and Astronautics; ldemasi@u.washington.edu. Member AIAA.

ϕ = small perturbation velocity potential
φ = angular coordinate
φ_d = angular coordinate which identifies the position of the generic doublet
Ψ = small perturbation acceleration potential
ψ = parameter used in the transformation of the coordinates (elliptical annular wings and arcs)
ψ_w = parameter which identifies the ellipse representing the annular wing
$2b_w$ = wing span, axis of the annular wing in the wing span direction
$\fint$ = integral defined in the Hadamard finite-part sense

Subscripts

$b_w/a_w = 1$ = related to the circular annular wing with $R_w = a_w = b_w$
$b_w/a_w > 1$ = related to the elliptical annular wing with $b_w > a_w$
$b_w/a_w < 1$ = related to the elliptical annular wing with $b_w < a_w$
d = referred to the doublet
opt = optimal conditions (minimum induced drag with fixed lift and wing span)
ref = referred to the classical cantilevered wing under optimal conditions
WTC = related to the wall tangency condition
w = referred to the wing

Superscript

$'$ = derivative of the function

Introduction

METHODS for induced-drag prediction and minimization have been pursued since the early days of aviation [1,2]. Reviews of procedures for induced-drag prediction can be found in the literature [3–6]. Optimal lift distributions for minimum drag on straight high-aspect ratio wings were obtained in the early years of the 20th century already, and interest in induced-drag minimization kept place with the evolution over the years of more complex wing configurations [7]. With the growing availability of digital computers and math programming algorithms, lifting surface/math programming optimum wing designs for minimum induced drag were reported first in the 1960s and early 1970s. Development of math programming based wing design for induced-drag minimization continued in the 1980s and 1990s, and the technology was applied to emerging unconventional wing configurations, such as the box wing and C-wing [3,8].

Some of the advantages of the math programming induced-drag minimization methods are that they are efficient and can be applied to general configurations subject to constraints of various types. The early analytical induced-drag minimization methods were applicable only to simple configurations with simple constraints. In this paper a theoretical approach for induced-drag minimization, first presented in [6], is applied to nonconventional nonplanar wing configurations. The method is based on a variational approach, and leads to a set of equations for the optimum solution directly. Under the hypotheses of steady incompressible and inviscid flow, the induced drag is minimized considering the wake to be rigid and aligned with the freestream velocity (a good overview of wake models can be found in the literature [9,10]).

The proposed method is not intended to replace math programming-based induced-drag minimization techniques. It complements such methods by shedding light on some of the analytical and numerical issues involved, and can provide benchmark test cases for the verification of accuracy and convergence characteristics of other minimization methods.

The present approach is based on an acceleration potential [11] formulation using doublets. For any doublet distribution the normalwash and induced drag can be found in a closed form. The induced drag or induced-drag coefficient are functionals to be minimized under fixed wing span and lift constraints. Using the techniques of the variational calculus [12–14] an Euler–Lagrange equation can be written. This equation in the present case is an integral equation (or a system of integral equations in the most general case) containing the unknown optimal doublet distribution. Hadamard finite-part integrals [15–18] in the formulation require special attention in the numerical solution process. In the following, known numerical results [19] are reproduced and new analytical formulations are presented. Annular wings (circular and elliptical) and elliptical lifting arcs are studied for all aspect ratios, and closed-form solutions for the optimal doublet distribution, normalwash, induced drag and efficiency are shown. To test the quality of solutions use is made of Munk's minimum induced drag theorem (MMIDT) [20]. The presented procedure is general and can be applied effectively to wings such as parabolic arcs, hyperbolic arcs, sinusoidal arcs, closed wing systems, C-wings, and general nonplanar wing configurations.

Euler–Lagrange Equation Involving Hadamard Finite-Part Integrals

A variational formulation of the induced-drag minimization problem leads to an Euler–Lagrange equation [12–14] where the integral has to be interpreted in the Hadamard finite-part sense [17]. Consider the following functional (which will be shown in subsequent sections to represent induced drag):

$$J = C_1 \int_{-1}^{+1} m(s) \left(\fint_{-1}^{+1} m(t) \bar{Y}(t,s)\, \mathrm{d}t \right) \mathrm{d}s \tag{1}$$

In Eq. (1) C_1 is a constant, the kernel $\bar{Y}(t,s)$ is a *symmetric* function (if t and s are switched the function does not change) which is *singular* when $t = s$. Suppose also that the order of the singularity is 2 and $m(-1) = m(+1) = 0$. In the most general case that has practical interest in the cases analyzed in this paper, the kernel can be written as a combination of a *regular symmetric* function ${}^{R}\bar{Y}(t,s)$ and a *singular symmetric* function ${}^{S}\bar{Y}(t,s)$ of order 2. Therefore, the kernel will be

$$\bar{Y}(t,s) = \bar{Y}(s,t) = {}^{R}\bar{Y}(t,s) + {}^{S}\bar{Y}(t,s) \tag{2}$$

For example, a possible kernel could be the following:

$$\bar{Y}(t,s) = \bar{Y}(s,t) = \frac{\sinh^2\psi_w \cosh^2\psi_w}{\{\sinh^2\psi_w + \sin^2[\pi(t+s)/2]\}^2} - \frac{\frac{1}{2}\cosh(2\psi_w)}{\{\sinh^2\psi_w + \sin^2[\pi(t+s)/2]\}} + \frac{1}{1-\cos[\pi(t-s)]} \tag{3}$$

where ψ_w is a known constant. In Eq. (3) the regular part of the kernel is represented by the first two terms, whereas the singular part is represented by the term $1/\{1-\cos[\pi(t-s)]\}$. The singular term can be manipulated to have the singularity in the form $1/[(t-s)^2]$. In this case (but this is valid for all functions which have singularity of order 2) this manipulation can be done multiplying and dividing by $(t-s)^2$:

$$\frac{1}{1-\cos[\pi(t-s)]} = \frac{(t-s)^2}{1-\cos[\pi(t-s)]} \frac{1}{(t-s)^2} \tag{4}$$

Notice that $[(t-s)^2]/\{1-\cos[\pi(t-s)]\}$ is *regular*. In fact, using the Taylor series it can be proven that

$$\lim_{t\to s} \frac{(t-s)^2}{1-\cos[\pi(t-s)]} = \frac{2}{\pi^2} \tag{5}$$

The singular term ${}^{S}\bar{Y}(t,s)$ can, then, be written as a product of a *known symmetric* function $g_1(t,s)$ (in the example $g_1(t,s) = [(t-s)^2]/\{1-\cos[\pi(t-s)]\}$) and the singular term $Y(t,s) = 1/[(t-s)^2]$:

$$ {}^{S}\bar{Y}(t,s) = g_1(t,s)Y(t,s) \tag{6} $$

Thus, the kernel has the expression

$$ \bar{Y}(t,s) = {}^{R}\bar{Y}(t,s) + g_1(t,s)Y(t,s) \tag{7} $$

Substituting Eq. (7) into Eq. (1), the functional can be written as

$$ J = C_1 \int_{-1}^{+1} m(s) \left(\oint_{-1}^{+1} m(t)[{}^{R}\bar{Y}(t,s) + g_1(t,s)Y(t,s)]\,\mathrm{d}t \right) \mathrm{d}s \tag{8} $$

or

$$ J = C_1 \int_{-1}^{+1} m(s) \left(\int_{-1}^{+1} m(t)\,{}^{R}\bar{Y}(t,s)\,\mathrm{d}t + \oint_{-1}^{+1} m(t) g_1(t,s) Y(t,s)\,\mathrm{d}t \right) \mathrm{d}s \tag{9} $$

Now, let the goal be to find a function $m(t)$ that minimizes J. Consider, also, a *constraint* of the following type:

$$ \bar{C} = C_2 \int_{-1}^{+1} m(t) g_2(t)\,\mathrm{d}t \tag{10} $$

where $\bar{C}$ is an assigned constant and $g_2(s)$ is a *known function*. The function m has to satisfy the boundary conditions (notice that $m_0 = m_1 = 0$)

$$ m(-1) = m_0, \qquad m(+1) = m_1 \tag{11} $$

Consider next a variation function $\delta_1(t)$ that satisfies the condition

$$ \delta_1(-1) = \delta_1(+1) = 0 \tag{12} $$

With this variation function, a solution for the problem can be found using the following relation (the subscript "opt" indicates the optimal condition: J is minimized):

$$ m(\cdot) = m_{\mathrm{opt}}(\cdot) + \sigma\delta_1(\cdot) \qquad \sigma \in (-1, 1) \tag{13} $$

In the preceding equation m satisfies the boundary conditions (11), if

$$ m_{\mathrm{opt}}(-1) = m_0, \qquad m_{\mathrm{opt}}(+1) = m_1 \tag{14} $$

Notice, also, that m_{opt} is the candidate function to minimize J. To apply the *Lagrange multiplier method* for optimization, constraint (10) is written as [6]

$$ c(t) = C_2 \int_{-1}^{t} m(s) g_2(s)\,\mathrm{d}s \Rightarrow c'(t) - C_2 m(t) g_2(t) = 0 \tag{15} $$

where

$$ c(+1) = \bar{C}, \qquad c(-1) = 0 \tag{16} $$

To apply the Lagrange multiplier method, the following steps must be taken [14]: first, substitute $m(\cdot) = m_{\mathrm{opt}}(\cdot) + \sigma\delta_1(\cdot)$ into the expression of J, and calculate the derivative with respect to σ. The derivative has to be evaluated for $\sigma = 0$.

Then, substitute $c(\cdot) = c(\cdot)_{\mathrm{opt}} + \sigma\delta_2(\cdot)$ and $m(\cdot) = m_{\mathrm{opt}}(\cdot) + \sigma\delta_1(\cdot)$ into Eq. (15). Notice that $\delta_2(+1) = \delta_2(-1) = 0$, $c_{\mathrm{opt}}(+1) = \bar{C}$, and $c_{\mathrm{opt}}(-1) = 0$. After the substitution, the derivative with respect to σ has to be calculated and evaluated for $\sigma = 0$. It can be shown (see Appendix A) that the resulting Euler–Lagrange equation is

$$ 2C_1 \int_{-1}^{+1} m_{\mathrm{opt}}(s)\,{}^{R}\bar{Y}(t,s)\,\mathrm{d}s + 2C_1 \oint_{-1}^{+1} m_{\mathrm{opt}}(s)\,{}^{S}\bar{Y}(t,s)\,\mathrm{d}s - C_2\lambda g_2(t) = 0 \tag{17} $$

Obviously, the constraint for the function m_{opt}

$$ \bar{C} = C_2 \int_{-1}^{+1} m_{\mathrm{opt}}(t) g_2(t)\,\mathrm{d}t \tag{18} $$

has to be satisfied as well as the Euler–Lagrange equation. The numerical solution of the Euler–Lagrange equation and the numerical quadrature of the Hadamard integrals are discussed in a previous paper [6]. To apply the numerical procedures described in Appendices B and C of [6], the Euler–Lagrange equation is written following Eq. (A11) (see Appendix A).

All the cases analyzed in this paper (annular wings and C-wings) will have the Euler–Lagrange equation in the form (17).

Brief Description of the Present Minimization Procedure

For incompressible, inviscid, small-perturbation steady flow, and with the wake considered rigid and aligned with the freestream velocity, it is possible to apply the following analytical procedure: first write the *small-perturbation acceleration potential* of the doublet distribution over the lifting line representing the wing. Let such distribution be called m.

The *small-perturbation velocity potential* is expressed by integration of the small-perturbation acceleration potential. This operation is essential for the imposition of the wall tangency condition (WTC).

The WTC is imposed next using Weissinger's approach. This approach is useful in the *direct problem*, i.e., this step allows one to calculate the doublet distribution when the twist distribution α is assigned. When the doublet distribution is calculated, the lift and induced drag can be determined. In this paper the direct approach is not discussed in detail [14,21].

Now, write the *normalwash* on the lifting line by calculating the derivative of the small-perturbation velocity potential with respect to the direction perpendicular the lifting line representing the lifting system. In the next step write the analytical expressions of the aerodynamic induced drag (which depends on the normalwash) and of the lifting force.

Then, derive the Euler–Lagrange equation: the induced drag has to be minimum with the constraints of fixed wing span and lift. Numerical (or analytical if possible) solution of the Euler–Lagrange equation follows, as well as the determination of the optimal doublet distribution m_{opt}. In the final two steps, calculate the efficiency of minimum induced drag and compare with a reference classical wing with the same wing span and total lift. Then check if the Munk's minimum induced drag theorem is satisfied (optional).

Aerodynamic Analysis of a Circular Annular Wing

Derivation of the Expression of the Small-Perturbation Acceleration Potential

The geometry of the wing is shown in Fig. 1. Considering the geometry of the wing it is clear that a convenient coordinate system is the following:

$$ \begin{aligned} y &= R\cos\varphi \quad 0 \le \varphi \le 2\pi \\ z &= R\sin\varphi \qquad R > 0 \end{aligned} \tag{19} $$

Using Eq. (19), each point of the space is uniquely defined by the coordinates x, R, and φ. The circular lifting line is placed in the plane y, z (at the first quarter according to Weissinger's approach). The points on the circular lifting line (radius R_w) representing the wing have coordinates y and z calculated using Eq. (19):

$$ \begin{aligned} y &= R_w\cos\varphi \quad 0 \le \varphi \le 2\pi \\ z &= R_w\sin\varphi \qquad R_w > 0 \end{aligned} \tag{20} $$

The geometry of the wing and the convention used are shown in Figs. 1 and 2. φ_d is the angular coordinate of the generic doublet positioned on the circular lifting line representing the wing. The small-perturbation acceleration potential of a doublet $M = m(s_d)\,\mathrm{d}s_d = m(\varphi_d)R_w\,\mathrm{d}\varphi_d$ positioned on the lifting line at the point corresponding to the curvilinear coordinate s_d (see Figs. 1 and 2) has expression

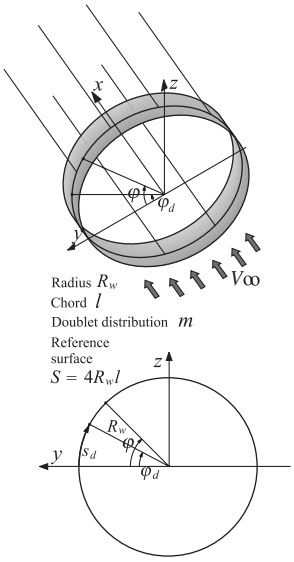

Fig. 1 Circular annular wing: reference coordinate system.

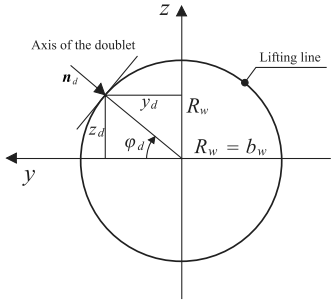

Fig. 2 Positive direction of the doublet's axis.

$$\mathrm{d}\,\Psi = -\frac{1}{4\pi} M \frac{n_{dx}(x - x_d) + n_{dy}(y - y_d) + n_{dz}(z - z_d)}{[(x - x_d)^2 + (y - y_d)^2 + (z - z_d)^2]^{\frac{3}{2}}} \tag{21}$$

where x_d, y_d, and z_d are the Cartesian coordinates of the point (defined by the curvilinear coordinate s_d) in which the doublet M is positioned. n_{dx}, n_{dy}, and n_{dz} are the components of the unit vector which defines the axis of the doublet M (see Fig. 2). Considering the fact that the lifting line is placed in the plane y, z (therefore $x_d = 0$) and remembering that the positive direction for the doublet is inward from the center (therefore $n_{dy} = -\cos\varphi_d$ and $n_{dz} = -\sin\varphi_d$), the contribution of the doublet M to the small-perturbation acceleration potential is

$$\begin{aligned}\mathrm{d}\Psi = -\frac{m(\varphi_d)}{4\pi} R_w [&-\cos\varphi_d (R\cos\varphi - R_w\cos\varphi_d) \\ &- \sin\varphi_d (R\sin\varphi - R_w\sin\varphi_d)]/\Delta^{\frac{3}{2}}\,\mathrm{d}\varphi_d\end{aligned} \tag{22}$$

where

$$\Delta = R_w^2 X^2 + R^2 + R_w^2 - 2RR_w\cos(\varphi - \varphi_d) \tag{23}$$

$$X = \frac{x}{R_w} \tag{24}$$

Note that in Eq. (22) the transformation of coordinates [Eqs. (19) and (20)] are used. Considering the *linearity* of the theory that is being developed, the small-perturbation acceleration potential of *all* doublets on the lifting line will be the integral over the circle (defined by R_w) of Eq. (22):

$$\Psi = \frac{1}{4\pi R_w^2}\int_0^{2\pi} \frac{m(\varphi_d)(R\cos(\varphi - \varphi_d) - R_w)}{[X^2 + R^2/R_w^2 + 1 - 2(R/R_w)\cos(\varphi - \varphi_d)]^{\frac{3}{2}}}\,\mathrm{d}\varphi_d \tag{25}$$

Expression of the Small-Perturbation Velocity Potential

To impose the boundary conditions, the *small-perturbation velocity potential* has to be written, integrating the expression of the small-perturbation acceleration potential:

$$\phi = \frac{R_w}{V_\infty}\int_{-\infty}^{X} \Psi\,\mathrm{d}\tau \tag{26}$$

where τ is a dummy variable (used to distinguish it from X). Substituting Eq. (25) into Eq. (26) and changing order of integration, the small-perturbation velocity potential becomes

$$\begin{aligned}\phi = \frac{1}{4\pi V_\infty R_w}\int_0^{2\pi} &\frac{m(\varphi_d)[R\cos(\varphi - \varphi_d) - R_w]}{R^2/R_w^2 + 1 - 2(R/R_w)\cos(\varphi - \varphi_d)} \\ &\times \left(\frac{X}{\sqrt{[X^2 + R^2/R_w^2 + 1 - 2(R/R_w)\cos(\varphi - \varphi_d)]}} + 1\right)\mathrm{d}\varphi_d\end{aligned} \tag{27}$$

WTC Using Weissinger's Approach

The WTC has to be imposed at the 3/4 chord point. Therefore, the WTC is imposed in

$$x_{\mathrm{WTC}} = \frac{l}{2} \Rightarrow X_{\mathrm{WTC}} = \frac{l}{2R_w} \tag{28}$$

The WTC is

$$-\alpha(\varphi) = \frac{1}{V_\infty}\left(\frac{1}{h_R}\frac{\partial\phi}{\partial R}\right)_{X = X_{\mathrm{WTC}}; R = R_w} \tag{29}$$

In the polar coordinate system [Eq. (19)] $h_R = 1$. Using Eq. (27) and calculating the derivative as prescribed in Eq. (29), the integral equation in the unknown doublet distribution (the twist distribution is assumed known) representing the mathematical imposition of the WTC is

$$\begin{aligned}-\alpha(\varphi) = &\frac{1}{4\pi V_\infty^2 R_w}\int_0^{2\pi}\left\{\frac{-m(\varphi_d)\cos(\varphi - \varphi_d)}{X_{\mathrm{WTC}} + \sqrt{X_{\mathrm{WTC}}^2 + 2[1 - \cos(\varphi - \varphi_d)]}}\right. \\ &\left.\times \frac{1}{\sqrt{X_{\mathrm{WTC}}^2 + 2[1 - \cos(\varphi - \varphi_d)]}}\right\}\mathrm{d}\varphi_d + \frac{1}{4\pi V_\infty^2 R_w} \\ &\times \int_0^{2\pi} m(\varphi_d)\left[-1 + \frac{1}{2}\left(\frac{X_{\mathrm{WTC}}}{\sqrt{X_{\mathrm{WTC}}^2 + 2[1 - \cos(\varphi - \varphi_d)]}}\right.\right. \\ &\left.\left. + 1\right)\right]\mathrm{d}\varphi_d + \frac{1}{4\pi V_\infty^2 R_w}\int_0^{2\pi} m(\varphi_d) \\ &\times \frac{1}{2} X_{\mathrm{WTC}} \frac{1 - \cos(\varphi - \varphi_d)}{\{\sqrt{X_{\mathrm{WTC}}^2 + 2[1 - \cos(\varphi - \varphi_d)]}\}^3}\,\mathrm{d}\varphi_d \\ &+ \frac{1}{4\pi V_\infty^2 R_w}\oint_0^{2\pi} \frac{m(\varphi_d)}{1 - \cos(\varphi - \varphi_d)}\,\mathrm{d}\varphi_d\end{aligned} \tag{30}$$

Normalwash $u_n(\varphi)$

Recalling the definition of the small-perturbation velocity potential, the normalwash is

$$u_n(\varphi) = \left(\frac{1}{h_R}\frac{\partial\phi}{\partial R}\right)_{R = R_w; X = 0} \tag{31}$$

This expression is formally similar to the expression used in Weissinger's condition [Eq. (29)]. Hence

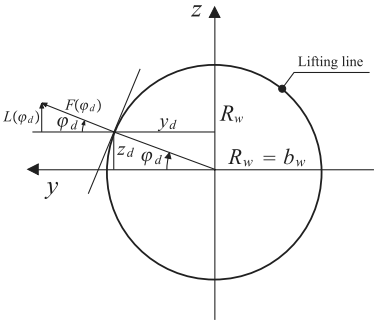

Fig. 3 Calculation of the lifting force.

$$u_n(\varphi) = \frac{1}{8\pi V_\infty R_w} \oint_0^{2\pi} \frac{m(\varphi_d)}{1 - \cos(\varphi - \varphi_d)}\, \mathrm{d}\varphi_d \tag{32}$$

The normalwash is positive when directed along $+R$ (outward the center of the circle). It is also possible [14] to calculate the normalwash via a geometric approach considering a distribution of circulation $\Gamma(\varphi)$ and integrating over the circle of all contributions of the vortices. Then, because the circulation and doublet distribution are coincident except for a multiplying constant [6] (the freestream velocity) and after integration by part, the expression (32) can be obtained.

Total Lifting Force

The selected positive direction of the doublet distribution is inward to the center, whereas the positive direction of the aerodynamic force per unit of length of arc is the radial direction. The force per unit of length in the direction of the doublet axis can be obtained [6] from the doublet distribution multiplying it by $-\rho_\infty$. Because the assumed positive direction of the force is radial (opposite to the direction of the doublet axis), it can be deduced that the aerodynamic force per unit of length is (see Fig. 3)

$$F(\varphi_d) = -[-\rho_\infty m(\varphi_d)] = \rho_\infty m(\varphi_d) \tag{33}$$

From Fig. 3, the *local lifting force per unit of length* is

$$L(\varphi_d) = F(\varphi_d) \sin\varphi_d = \rho_\infty m(\varphi_d) \sin\varphi_d \tag{34}$$

The total lifting force is obtained by integrating Eq. (34) over the lifting line:

$$L = \int_0^{2\pi} L(\varphi_d) R_w\, \mathrm{d}\varphi_d = \rho_\infty R_w \int_0^{2\pi} m(\varphi_d) \sin\varphi_d\, \mathrm{d}\varphi_d \tag{35}$$

The coefficient of lift (reference surface defined as $S = 4R_w l$) is

$$C_L = \frac{L}{\frac{1}{2}\rho_\infty (4R_w l) V_\infty^2} = \frac{1}{2lV_\infty^2} \int_0^{2\pi} m(\varphi_d) \sin\varphi_d\, \mathrm{d}\varphi_d \tag{36}$$

Evaluation of the Induced Drag

The induced drag per unit of length of arc is the product of the aerodynamic force $F(\varphi_d)$ per unit of length of arch and the trigonometric tangent of the induced incidence $\alpha_i(\varphi_d)$. Assuming small perturbations,

$$D_i(\varphi_d) = F(\varphi_d) \tan[\alpha_i(\varphi_d)] \simeq F(\varphi_d)\alpha_i(\varphi_d) \tag{37}$$

Using the expressions of the induced incidence $\alpha_i(\varphi_d) = -[u_n(\varphi_d)]/V_\infty$ and aerodynamic force $F(\varphi_d) = \rho_\infty m(\varphi_d)$, the induced drag per unit of length is

$$D_i(\varphi_d) = -\rho_\infty m(\varphi_d) \frac{u_n(\varphi_d)}{V_\infty} \tag{38}$$

The total induced drag can be obtained by integration over the circle [see Eq. (32)]. As it will be explained later when the induced drag is minimized, the case in which the doublet distribution m is zero at both the endpoints of the integral will be analyzed. This guarantees that the external internal is a standard integral and that the singularity of the inner integral is always internal and so the standard linear change of variable rule is allowed [17]. Thus,

$$D_i = -\frac{\rho_\infty}{8\pi V_\infty^2} \int_0^{2\pi} m(\varphi) \left(\oint_0^{2\pi} \frac{m(\varphi_d)}{1 - \cos(\varphi_d - \varphi)}\, \mathrm{d}\varphi_d \right) \mathrm{d}\varphi \tag{39}$$

The coefficient of induced drag is

$$C_{D_i} = -\frac{1}{16R_w l\pi V_\infty^4} \int_0^{2\pi} m(\varphi) \left(\oint_0^{2\pi} \frac{m(\varphi_d)}{1 - \cos(\varphi_d - \varphi)}\, \mathrm{d}\varphi_d \right) \mathrm{d}\varphi \tag{40}$$

Aerodynamic Analysis of an Elliptical Annular Wing with $b_w > a_w$

The procedure used for the circular annular wing can be adopted for the elliptical annular wing as well.

Derivation of the Expression of the Small-Perturbation Acceleration Potential

The geometry and the notation are shown in Fig. 4. Because of the particular geometry of the lifting line, a good choice of coordinate system can be represented by the relation

$$\begin{aligned} y &= c \cosh\psi \cos\varphi \quad 0 \le \varphi \le 2\pi \\ z &= c \sinh\psi \sin\varphi \qquad \psi > 0 \end{aligned} \tag{41}$$

Using Eq. (41) and Fig. 5, it is clear that each point in a plane parallel to the plane which contains the wing is uniquely determined as the intersection of an ellipse (each curve with $\psi = \text{const}$ is an ellipse) and a hyperbola (each curve with $\varphi = \text{const}$ is a hyperbola). At each intersection of an ellipse and a hyperbola, the tangent of the ellipse is perpendicular to the tangent of the hyperbola. The *ellipse representing the lifting line* is obtained by setting $\psi = \psi_w$ (as in the circular wing the wing was obtained setting $R = R_w$). Therefore, the points on the wing have the coordinates y and z given by the following formula:

$$\begin{aligned} y &= c \cosh\psi_w \cos\varphi \quad 0 \le \varphi \le 2\pi \\ z &= c \sinh\psi_w \sin\varphi \qquad \psi_w > 0 \end{aligned} \tag{42}$$

It can observed that the semiaxes a_w and b_w are

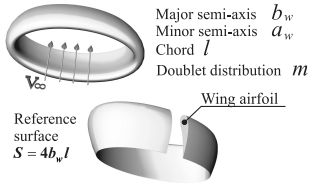

Fig. 4 Elliptical annular wing with $b_w > a_w$.

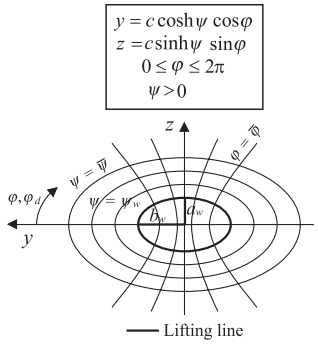

Fig. 5 Transformation of the coordinate system.

$$a_w = c\sinh\psi_w \qquad b_w = c\cosh\psi_w \tag{43}$$

Using Eq. (43),

$$c^2 = b_w^2 - a_w^2 \qquad \cosh^2\psi_w = \frac{b_w^2}{b_w^2 - a_w^2} \tag{44}$$

From Eq. (41),

$$\begin{aligned} \mathrm{d}s^2 &= \mathrm{d}y^2 + \mathrm{d}z^2 = c^2(\cosh^2\psi - \cos^2\varphi)(\mathrm{d}\psi^2 + \mathrm{d}\varphi^2) \\ &= h^2(\mathrm{d}\psi^2 + \mathrm{d}\varphi^2) \end{aligned} \tag{45}$$

On the ellipse representing the lifting line ($\psi = \psi_w = \text{const} \Rightarrow \mathrm{d}\psi = 0$), the infinitesimal arc has the following length (see Eq. (45); the definition $h_{w\varphi_d} = \sqrt{\cosh^2\psi_w - \cos^2\varphi_d}$ is also used):

$$\mathrm{d}\,s_d = c\sqrt{\cosh^2\psi_w - \cos^2\varphi_d}\,\mathrm{d}\varphi_d = c h_{w\varphi_d}\,\mathrm{d}\varphi_d \tag{46}$$

Thus, the generic doublet M positioned at a point on the ellipse has the following expression:

$$\begin{aligned} M &= m(s_d)\mathrm{d}s_d = m(\varphi_d)c\sqrt{\cosh^2\psi_w - \cos^2\varphi_d}\,\mathrm{d}\varphi_d \\ &= m(\varphi_d)c h_{w\varphi_d}\,\mathrm{d}\varphi_d \end{aligned} \tag{47}$$

Considering Eq. (21), using the new coordinate system [Eqs. (41) and (42)], and integrating over the ellipse, the small-perturbation acceleration potential can be written as

$$\Psi = \frac{1}{8\pi c}\int_0^{2\pi} m(\varphi_d)\frac{H_3}{H_4^{3/2}}\,\mathrm{d}\varphi_d \tag{48}$$

where

$$\begin{aligned} X &= \frac{x}{c} \\ H_3 &= \sinh(\psi + \psi_w)\cos(\varphi - \varphi_d) - \sinh(\psi - \psi_w)\cos(\varphi + \varphi_d) \\ &\quad - \sinh 2\psi_w \\ H_4 &= X^2 + \sinh^2\psi + \cos^2\varphi - \cosh(\psi - \psi_w)\cos(\varphi + \varphi_d) \\ &\quad - \cosh(\psi + \psi_w)\cos(\varphi - \varphi_d) + \sinh^2\psi_w + \cos^2\varphi_d \end{aligned}$$

The doublet axes are chosen as in the case of the circular annular wing: they act toward the local center of curvature.

Small-Perturbation Velocity Potential

Integrating the small-perturbation acceleration potential, it is possible to obtain the small-perturbation velocity potential. After the integration is performed, the result is

$$\phi = \frac{1}{8\pi V_\infty}\int_0^{2\pi} m(\varphi_d)\frac{H_3}{H_4 - X^2}\left(\frac{X}{\sqrt{H_4}} + 1\right)\mathrm{d}\varphi_d \tag{49}$$

This expression is useful in the imposition of Weissinger's condition.

WTC Using Weissinger's Approach

The WTC is imposed in

$$x_{\mathrm{WTC}} = \frac{l}{2} \Rightarrow X_{\mathrm{WTC}} = \frac{l}{2c} \tag{50}$$

The direction perpendicular to the generic ellipse of the coordinate system is represented by ψ. Thus, the WTC is

$$-\alpha(\varphi) = \frac{1}{V_\infty}\left(\frac{1}{h}\frac{\partial\phi}{\partial\psi}\right)_{X = X_{\mathrm{WTC}};\psi = \psi_w} \tag{51}$$

Notice that in the adopted coordinate system $h = c\sqrt{\cosh^2\psi - \cos^2\varphi}$ [see Eq. (45)]. Using Eq. (49) and calculating the derivative as prescribed in Eq. (51), the integral equation in the unknown doublet distribution (the twist distribution is assumed known) representing the mathematical imposition of the WTC is

$$\begin{aligned} -\alpha(\varphi) = \frac{1}{8\pi c V_\infty^2 h_{w\varphi}}\Bigg(&\int_0^{2\pi} m(\varphi_d)(T_1 + T_2 + T_3)\,\mathrm{d}\varphi_d \\ &+ 2\fint_0^{2\pi}\frac{m(\varphi_d)}{1 - \cos(\varphi - \varphi_d)}\,\mathrm{d}\varphi_d\Bigg) \end{aligned} \tag{52}$$

where

$$\begin{aligned} h_{w\varphi} &= \sqrt{\cosh^2\psi_w - \cos^2\varphi} \\ T_1 &= \frac{X_{\mathrm{WTC}}\cosh^2\psi_w\sinh^2\psi_w[1 - \cos(\varphi - \varphi_d)]}{(H_5)(H_6)^{\frac{3}{2}}} \\ T_2 &= \frac{\cosh^2\psi_w\cos(\varphi - \varphi_d) - \cos\varphi\cos\varphi_d}{(H_5)}H_7 - \frac{\cosh(2\psi_w)}{(H_5)} \\ T_3 &= \frac{\sinh^2\psi_w\cosh^2\psi_w}{(H_5)^2}\left(\frac{X_{\mathrm{WTC}}}{\sqrt{H_6}} + 1\right) \\ H_7 &= \frac{-2(H_5)}{(X_{\mathrm{WTC}} + \sqrt{H_6})\sqrt{H_6}} \qquad H_5 = \sinh^2\psi_w + \sin^2\frac{\varphi + \varphi_d}{2} \\ H_6 &= X_{\mathrm{WTC}}^2 + 2\left(\sinh^2\psi_w + \sin^2\frac{\varphi + \varphi_d}{2}\right)[1 - \cos(\varphi - \varphi_d)] \end{aligned} \tag{53}$$

Normalwash $u_n(\varphi)$

Using the definition of the small-perturbation velocity potential, the normalwash is

$$u_n(\varphi) = \left(\frac{1}{h}\frac{\partial\phi}{\partial\psi}\right)_{\psi = \psi_w;X = 0} \tag{54}$$

Introducing the definitions

$$\begin{aligned} \mathcal{A}(\varphi, \varphi_d) &= \frac{\sinh^2\psi_w\cosh^2\psi_w}{\{\sinh^2\psi_w + \sin^2[(\varphi + \varphi_d)/2]\}^2} \\ \mathcal{B}(\varphi, \varphi_d) &= \frac{\frac{1}{2}\cosh(2\psi_w)}{\sinh^2\psi_w + \sin^2[(\varphi + \varphi_d)/2]} \end{aligned} \tag{55}$$

the normalwash can be written as

$$\begin{aligned} u_n(\varphi) = &\frac{1}{8\pi c V_\infty h_{w\varphi}}\int_0^{2\pi} m(\varphi_d)[\mathcal{A}(\varphi, \varphi_d) - \mathcal{B}(\varphi, \varphi_d)]\,\mathrm{d}\varphi_d \\ &+ \frac{1}{8\pi c V_\infty h_{w\varphi}}\fint_0^{2\pi}\frac{m(\varphi_d)}{1 - \cos(\varphi - \varphi_d)}\,\mathrm{d}\varphi_d \end{aligned} \tag{56}$$

Total Lifting Force

Based on the convention for the positive sign of the doublet axis, the aerodynamic force, which acts outward from the local center of curvature, has the expression given in Eq. (33). The local normal direction is the aerodynamic force direction. The expression of the unit vector which acts outward from the local center of curvature is

$$\boldsymbol{N}_d = -\boldsymbol{n}_d = \frac{\cos\varphi_d\sinh\psi_w}{h_{w\varphi_d}}\boldsymbol{j} + \frac{\sin\varphi_d\cosh\psi_w}{h_{w\varphi_d}}\boldsymbol{k} \tag{57}$$

$\boldsymbol{N}_d$ has modulus one. Thus, the z-component represents the quantity $\sin\beta$ (see Fig. 6):

$$\sin\beta = (\boldsymbol{N}_d)_z = \frac{\sin\varphi_d\cosh\psi_w}{h_{w\varphi_d}} \tag{58}$$

The *local* lift is

$$L(\varphi_d) = F(\varphi_d)\sin\beta = \rho_\infty m(\varphi_d)\frac{\cosh\psi_w\sin\varphi_d}{h_{w\varphi_d}} \tag{59}$$

Using Eq. (46) and the relation $c\cosh\psi_w = b_w$, and after integration over the lifting line, the total lifting force is

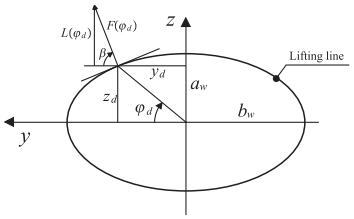

Fig. 6 Calculation of the lifting force.

$$L = c\int_0^{2\pi} L(\varphi_d)h_{w\varphi_d}\,\mathrm{d}\varphi_d = \rho_\infty b_w \int_0^{2\pi} m(\varphi_d)\sin\varphi_d\,\mathrm{d}\varphi_d \tag{60}$$

The coefficient of lift is

$$C_L = \frac{L}{\frac{1}{2}\rho_\infty V_\infty^2 4b_w l} = \frac{1}{2V_\infty^2 l}\int_0^{2\pi} m(\varphi_d)\sin\varphi_d\,\mathrm{d}\varphi_d \tag{61}$$

Evaluation of the Induced Drag

The induced drag is found using the same procedure adopted for the circular annular wing (as for the circular wing we focus on the case in which the doublet distribution m is zero at the endpoints of the integral):

$$D_i = \int_0^{2\pi} \rho_\infty m(\varphi_d)\left(-\frac{u_n(\varphi_d)}{V_\infty}\right)ch_{w\varphi_d}\,\mathrm{d}\varphi_d \tag{62}$$

Substitution of the expression of the normalwash [Eq. (56)],

$$\begin{aligned} D_i = &-\frac{\rho_\infty}{8\pi V_\infty^2}\int_0^{2\pi} m(\varphi)\int_0^{2\pi} m(\varphi_d)[\mathcal{A}(\varphi,\varphi_d)-\mathcal{B}(\varphi,\varphi_d)]\,\mathrm{d}\varphi_d\,\mathrm{d}\varphi \\ &-\frac{\rho_\infty}{8\pi V_\infty^2}\int_0^{2\pi} m(\varphi)\,\text{⨍}_0^{2\pi}\frac{m(\varphi_d)}{1-\cos(\varphi-\varphi_d)}\,\mathrm{d}\varphi_d\,\mathrm{d}\varphi \end{aligned} \tag{63}$$

The coefficient of induced drag is obtained after dividing the preceding expression by $\frac{1}{2}\rho_\infty V_\infty^2 4b_w l$:

$$\begin{aligned} C_{D_i} = &-\frac{1}{16\pi b_w l V_\infty^4}\int_0^{2\pi} m(\varphi)\int_0^{2\pi} m(\varphi_d)[\mathcal{A}(\varphi,\varphi_d) \\ &-\mathcal{B}(\varphi,\varphi_d)]\,\mathrm{d}\varphi_d\,\mathrm{d}\varphi - \frac{1}{16\pi b_w l V_\infty^4} \\ &\times\int_0^{2\pi} m(\varphi)\,\text{⨍}_0^{2\pi}\frac{m(\varphi_d)}{1-\cos(\varphi-\varphi_d)}\,\mathrm{d}\varphi_d\,\mathrm{d}\varphi \end{aligned} \tag{64}$$

Aerodynamic Analysis of an Elliptical Annular Wing with $b_w < a_w$

Because the same procedure used for the preceding cases is adopted for an ellipse with $b_w < a_w$, only the principal relations are reported.

Derivation of the Expression of the Small-Perturbation Acceleration Potential

The coordinate system is slightly different than the system adopted in the case of elliptical annular wing with $b_w > a_w$. In particular, the transformation is

$$\begin{aligned} y &= c\sinh\psi\cos\varphi \quad 0\le\varphi\le 2\pi \\ z &= c\cosh\psi\sin\varphi \qquad \psi > 0 \end{aligned} \tag{65}$$

The ellipse with semiaxes a_w and b_w is obtainable when

$$a_w = c\cosh\psi_w \qquad b_w = c\sinh\psi_w \tag{66}$$

From the last equations,

$$c^2 = a_w^2 - b_w^2 \qquad \cosh^2\psi_w = \frac{a_w^2}{a_w^2-b_w^2} \qquad \sinh^2\psi_w = \frac{b_w^2}{a_w^2-b_w^2} \tag{67}$$

The ellipse representing the lifting line is

$$\begin{aligned} y &= c\sinh\psi_w\cos\varphi \quad 0\le\varphi\le 2\pi \\ z &= c\cosh\psi_w\sin\varphi \qquad \psi_w > 0 \end{aligned} \tag{68}$$

As has been done for the case in which $b_w > a_w$, it is possible to find the relation

$$\begin{aligned} \mathrm{d}s^2 &= \mathrm{d}y^2 + \mathrm{d}z^2 = c^2(\sinh^2\psi + \cos^2\varphi)(\mathrm{d}\psi^2 + \mathrm{d}\varphi^2) \\ &= \bar{h}^2(\mathrm{d}\psi^2 + \mathrm{d}\varphi^2) \end{aligned} \tag{69}$$

Now consider the ellipse w. It is possible to show that the infinitesimal arc has the dimension (the definition $\bar{h}_{w\varphi_d} = \sqrt{\sinh^2\psi_w + \cos^2\varphi_d}$ is used)

$$\mathrm{d}\,s_d = c\sqrt{\sinh^2\psi_w + \cos^2\varphi_d}\,\mathrm{d}\varphi_d = c\bar{h}_{w\varphi_d}\,\mathrm{d}\varphi_d \tag{70}$$

The small-perturbation acceleration potential has equation

$$\Psi = \frac{1}{8\pi c}\int_0^{2\pi} m(\varphi_d)\frac{\bar{H}_3}{\bar{H}_4^{\frac{3}{2}}}\,\mathrm{d}\varphi_d \tag{71}$$

where

$$\begin{aligned} \bar{H}_3 &= \sinh(\psi+\psi_w)\cos(\varphi-\varphi_d) + \sinh(\psi-\psi_w)\cos(\varphi+\varphi_d) \\ &\quad -\sinh 2\psi_w \\ \bar{H}_4 &= X^2 + \sinh^2\psi + \sin^2\varphi + \sinh^2\psi_w + \sin^2\varphi_d \\ &\quad -\cosh(\psi+\psi_w)\cos(\varphi-\varphi_d) + \cosh(\psi-\psi_w)\cos(\varphi+\varphi_d) \end{aligned}$$

Small-Perturbation Velocity Potential

The small-perturbation velocity potential is

$$\phi = \frac{1}{8\pi V_\infty}\int_0^{2\pi} m(\varphi_d)\frac{\bar{H}_3}{\bar{H}_4 - X^2}\left(\frac{X}{\sqrt{\bar{H}_4}}+1\right)\mathrm{d}\varphi_d \tag{72}$$

WTC Using Weissinger's Approach

Using Weissinger's approach, the integral equation in the unknown doublet distribution can be written as

$$\begin{aligned} -\alpha(\varphi) = &\frac{1}{8\pi c V_\infty^2 \bar{h}_{w\varphi}}\left(\int_0^{2\pi} m(\varphi_d)(\bar{T}_1+\bar{T}_2+\bar{T}_3)\,\mathrm{d}\varphi_d\right. \\ &\left. +2\,\text{⨍}_0^{2\pi}\frac{m(\varphi_d)}{1-\cos(\varphi-\varphi_d)}\,\mathrm{d}\varphi_d\right) \end{aligned} \tag{73}$$

where

$$\begin{aligned} \bar{h}_{w\varphi} &= \sqrt{(\sinh^2\psi_w + \cos^2\varphi)} \\ \bar{T}_1 &= \frac{X_{\mathrm{WTC}}\cosh^2\psi_w\sinh^2\psi_w[1-\cos(\varphi-\varphi_d)]}{(\bar{H}_5)(\bar{H}_6)^{\frac{3}{2}}} \\ \bar{T}_2 &= \frac{\cosh^2\psi_w\cos(\varphi-\varphi_d) - \sin\varphi\sin\varphi_d}{(\bar{H}_5)}\bar{H}_7 - \frac{\cosh(2\psi_w)}{(\bar{H}_5)} \\ \bar{T}_3 &= \frac{\sinh^2\psi_w\cosh^2\psi_w}{(\bar{H}_5)^2}\left(\frac{X_{\mathrm{WTC}}}{\sqrt{\bar{H}_6}}+1\right) \\ \bar{H}_7 &= \frac{-2(\bar{H}_5)}{(X_{\mathrm{WTC}}+\sqrt{\bar{H}_6})\sqrt{\bar{H}_6}} \qquad \bar{H}_5 = \sinh^2\psi_w + \cos^2\frac{\varphi+\varphi_d}{2} \\ \bar{H}_6 &= X_{\mathrm{WTC}}^2 + 2\left(\sinh^2\psi_w + \cos^2\frac{\varphi+\varphi_d}{2}\right)[1-\cos(\varphi-\varphi_d)] \end{aligned} \tag{74}$$

Normalwash $u_n(\varphi)$

Introducing the definitions

$$\bar{\mathcal{A}}(\varphi,\varphi_d)=\frac{\sinh^2\psi_w\cosh^2\psi_w}{\{\sinh^2\psi_w+\cos^2[(\varphi+\varphi_d)/2]\}^2}$$
$$\bar{\mathcal{B}}(\varphi,\varphi_d)=\frac{\frac{1}{2}\cosh(2\psi_w)}{\sinh^2\psi_w+\cos^2[(\varphi+\varphi_d)/2]} \tag{75}$$

the normalwash can be demonstrated to be

$$u_n(\varphi)=\frac{1}{8\pi cV_\infty\bar{h}_{w\varphi}}\int_0^{2\pi}m(\varphi_d)[\bar{\mathcal{A}}(\varphi,\varphi_d)-\bar{\mathcal{B}}(\varphi,\varphi_d)]\,\mathrm{d}\varphi_d$$
$$+\frac{1}{8\pi cV_\infty\bar{h}_{w\varphi}}\oint_0^{2\pi}\frac{m(\varphi_d)}{1-\cos(\varphi-\varphi_d)}\,\mathrm{d}\varphi_d \tag{76}$$

Total Lifting Force

The aerodynamic force, which acts outward from the local center of curvature, has the expression given in Eq. (33). The local normal direction is the aerodynamic force direction. The expression of the unit vector which acts outward from the local center of curvature is

$$\boldsymbol{N}_d=-\boldsymbol{n}_d=\frac{\cos\varphi_d\cosh\psi_w}{\bar{h}_{w\varphi_d}}\boldsymbol{j}+\frac{\sin\varphi_d\sinh\psi_w}{\bar{h}_{w\varphi_d}}\boldsymbol{k} \tag{77}$$

Thus

$$\sin\beta=(N_d)_z=\frac{\sin\varphi_d\sinh\psi_w}{\bar{h}_{w\varphi_d}} \tag{78}$$

The *local* lift is

$$L(\varphi_d)=F(\varphi_d)\sin\beta=\rho_\infty m(\varphi_d)\frac{\sinh\psi_w\sin\varphi_d}{\bar{h}_{w\varphi_d}} \tag{79}$$

Using the relations $\mathrm{d}s_d=c\bar{h}_{w\varphi_d}\,\mathrm{d}\varphi_d$ and $c\sinh\psi_w=b_w$, integrating over the lifting line, the total lifting force is

$$L=c\int_0^{2\pi}L(\varphi_d)\bar{h}_{w\varphi_d}\,\mathrm{d}\varphi_d=\rho_\infty b_w\int_0^{2\pi}m(\varphi_d)\sin\varphi_d\,\mathrm{d}\varphi_d \tag{80}$$

The coefficient of lift is

$$C_L=\frac{L}{\frac{1}{2}\rho_\infty V_\infty^2 4b_w l}=\frac{1}{2V_\infty^2 l}\int_0^{2\pi}m(\varphi_d)\sin\varphi_d\,\mathrm{d}\varphi_d \tag{81}$$

Evaluation of the Induced Drag

The induced drag has expression (as for the circular wing we focus on the case in which the doublet distribution m is zero at the endpoints of the integral)

$$D_i=\int_0^{2\pi}\rho_\infty m(\varphi_d)\left(-\frac{u_n(\varphi_d)}{V_\infty}\right)c\bar{h}_{w\varphi_d}\,\mathrm{d}\varphi_d \tag{82}$$

Substituting the expression of the normalwash,

$$D_i=-\frac{\rho_\infty}{8\pi V_\infty^2}\int_0^{2\pi}m(\varphi)\int_0^{2\pi}m(\varphi_d)[\bar{\mathcal{A}}(\varphi,\varphi_d)-\bar{\mathcal{B}}(\varphi,\varphi_d)]\,\mathrm{d}\varphi_d\,\mathrm{d}\varphi$$
$$-\frac{\rho_\infty}{8\pi V_\infty^2}\int_0^{2\pi}m(\varphi)\oint_0^{2\pi}\frac{m(\varphi_d)}{1-\cos(\varphi-\varphi_d)}\,\mathrm{d}\varphi_d\,\mathrm{d}\varphi \tag{83}$$

The coefficient of induced drag is

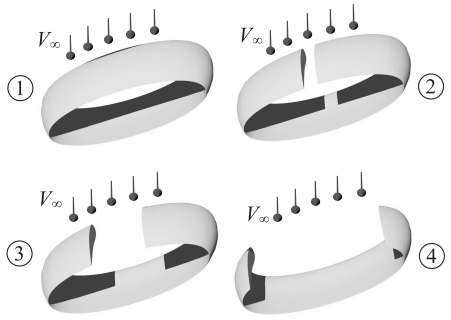

Fig. 7 Elliptical annular wing and elliptical lifting arcs.

$$C_{D_i}=-\frac{1}{16\pi b_w l V_\infty^4}\int_0^{2\pi}m(\varphi)\int_0^{2\pi}m(\varphi_d)[\bar{\mathcal{A}}(\varphi,\varphi_d)$$
$$-\bar{\mathcal{B}}(\varphi,\varphi_d)]\,\mathrm{d}\varphi_d\,\mathrm{d}\varphi-\frac{1}{16\pi b_w l V_\infty^4}$$
$$\times\int_0^{2\pi}m(\varphi)\oint_0^{2\pi}\frac{m(\varphi_d)}{1-\cos(\varphi-\varphi_d)}\,\mathrm{d}\varphi_d\,\mathrm{d}\varphi \tag{84}$$

Aerodynamic Analysis of Elliptical Lifting Arcs

It is interesting to compare C-wings and closed wing systems (see Fig. 7) using the theoretical technique exposed in the preceding sections. Particularly useful is the comparison between the elliptical annular wing and the corresponding arcs (see Fig. 7). The elliptical lifting arcs are useful to describe the physical behavior of C-wings and winglets. However, other aspects of the design (aeroelasticity, for example) should be taken into account when studying a wing system [3].

Convex Elliptical Lifting Arcs

The convex elliptical lifting arcs (see Fig. 8) can be studied similarly, as has been done for the other wings. This means using a doublet distribution, writing the small-perturbation acceleration potential, imposing Weissinger's condition and finding the integral equation. But there is a simple way to achieve the same goal: the same equations (appropriately modified) used for the corresponding annular wings can be used. Using the linearity of the equations, it can be easily seen that the difference between the annular wings and their arcs obtained from them is (from a mathematical point of view) only in the integration domain. However, the doublet distribution has to be zero at the tips of the wing and this does not happen, in the most general case, in the closed-wing systems. This fact allows one to write the external integral of the coefficient of the induced drag as a standard integral. Consider an elliptical annular wing with $b_w > a_w$. Referring to Fig. 8, it is clear that the lift and induced drag have expressions [see Eqs. (60) and (63)]

$$L=\rho_\infty b_w\int_{\beta_1}^{\beta_2}m(\varphi_d)\sin\varphi_d\,\mathrm{d}\varphi_d \tag{85}$$

$$D_i=-\frac{\rho_\infty}{8\pi V_\infty^2}\int_{\beta_1}^{\beta_2}m(\varphi)\int_{\beta_1}^{\beta_2}m(\varphi_d)[\mathcal{A}(\varphi,\varphi_d)-\mathcal{B}(\varphi,\varphi_d)]\,\mathrm{d}\varphi_d\,\mathrm{d}\varphi$$
$$-\frac{\rho_\infty}{8\pi V_\infty^2}\int_{\beta_1}^{\beta_2}m(\varphi)\oint_{\beta_1}^{\beta_2}\frac{m(\varphi_d)}{1-\cos(\varphi-\varphi_d)}\,\mathrm{d}\varphi_d\,\mathrm{d}\varphi \tag{86}$$

where (see Fig. 8)

$$\beta_1=\frac{3}{2}\pi-\varepsilon\pi\qquad\beta_2=\frac{3}{2}\pi+\varepsilon\pi \tag{87}$$

Notice that the doublets' axes are directed toward the local center as the corresponding annular wing. In the case of arcs that come from an ellipse with $b_w < a_w$, the expression of the lift is still Eq. (85) and the induced drag is

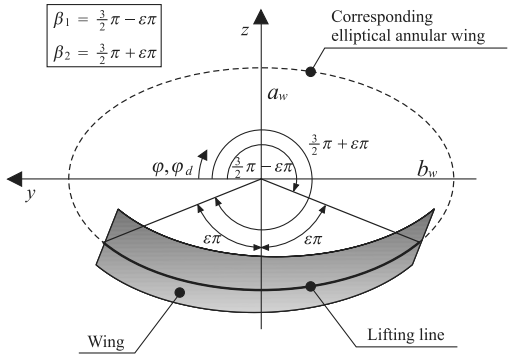

Fig. 8 Convex elliptical lifting arcs. Geometry and notations.

$$D_i = -\frac{\rho_\infty}{8\pi V_\infty^2}\int_{\beta_1}^{\beta_2} m(\varphi)\int_{\beta_1}^{\beta_2} m(\varphi_d)[\bar{\mathcal{A}}(\varphi,\varphi_d) - \bar{\mathcal{B}}(\varphi,\varphi_d)]\,\mathrm{d}\varphi_d\,\mathrm{d}\varphi - \frac{\rho_\infty}{8\pi V_\infty^2}\int_{\beta_1}^{\beta_2} m(\varphi)\,\Xint=_{\beta_1}^{\beta_2} \frac{m(\varphi_d)}{1-\cos(\varphi-\varphi_d)}\,\mathrm{d}\varphi_d\,\mathrm{d}\varphi \tag{88}$$

In the case of arcs that come from a circular (in which $R_w = b_w$), the induced drag is

$$D_i = -\frac{\rho_\infty}{8\pi V_\infty^2}\int_{\beta_1}^{\beta_2} m(\varphi)\,\Xint=_{\beta_1}^{\beta_2} \frac{m(\varphi_d)}{1-\cos(\varphi-\varphi_d)}\,\mathrm{d}\varphi_d\,\mathrm{d}\varphi \tag{89}$$

and the lift is still obtained using Eq. (85). The coefficients of lift and induced drag are obtained dividing the lift and induced drag by $\frac{1}{2}\rho_\infty V_\infty^2 S$, where S is a reference surface. S can be chosen as the projection of the wing on plane x–y:

$$\begin{aligned} S &= 2lb_w\sin(\varepsilon\pi) \quad \text{if } \varepsilon < \tfrac{1}{2} \\ S &= 2lb_w \qquad\quad \text{if } \varepsilon \geq \tfrac{1}{2} \end{aligned} \tag{90}$$

S can also be chosen to be equal to $4b_w l$, to have an easy comparison with the elliptical annular wing.

Concave Elliptical Lifting Arcs

The concave elliptical lifting arcs (see Fig. 9) can be studied similarly, as in the preceding section. Formally, Eqs. (85), (86), (88), and (89) are still valid. Only the definitions of β_1 and β_2 (see Fig. 9) are different:

$$\beta_1 = \frac{\pi}{2} - \varepsilon\pi \qquad \beta_2 = \frac{\pi}{2} + \varepsilon\pi \tag{91}$$

Transformation of the Variables

Several wing systems have been analyzed so far: annular wings and arcs (C-wings). To solve the equations numerically, it is convenient to change the variables to have all integrals with limits -1 and $+1$. In all cases examined here the singularity is internal to the interval of integration. Therefore the changing of variables, in the Hadamard integrals, is possible without adding extra terms [17]. For each of the case, the expressions of the coefficient of lift and induced drag is rewritten in the new coordinates.

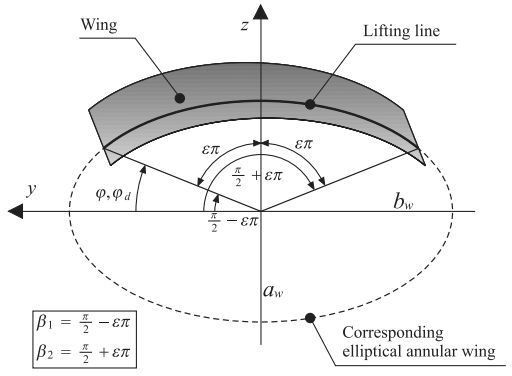

Fig. 9 Concave elliptical lifting Arcs. Geometry and notations.

Circular Annular Wing

The following transformation is used:

$$\varphi_d = \pi(t+1) \qquad \varphi = \pi(s+1) \tag{92}$$

The coefficients of lift and induced drag are

$$C_L = -\frac{\pi}{2V_\infty^2 l}\int_{-1}^{+1} m(t)\sin(\pi t)\,\mathrm{d}t \tag{93}$$

$$C_{D_i} = -\frac{\pi}{16R_w l V_\infty^4}\int_{-1}^{+1} m(s)\left(\Xint=_{-1}^{+1} \frac{m(t)}{1-\cos[\pi(t-s)]}\,\mathrm{d}t\right)\mathrm{d}s \tag{94}$$

Elliptical Annular Wing with $b_w > a_w$

The transformation used is presented in Eq. (92). The coefficient of lift is expressed by Eq. (93). The coefficient of induced drag is

$$C_{D_i} = -\frac{\pi}{16b_w l V_\infty^4}\int_{-1}^{+1} m(s)\int_{-1}^{+1} m(t)[\mathcal{A}(t,s) - \mathcal{B}(t,s)]\,\mathrm{d}t\,\mathrm{d}s - \frac{\pi}{16b_w l V_\infty^4}\int_{-1}^{+1} m(s)\,\Xint=_{-1}^{+1} \frac{m(t)}{1-\cos[\pi(t-s)]}\,\mathrm{d}t\,\mathrm{d}s \tag{95}$$

where

$$\begin{aligned} \mathcal{A}(t,s) &= \frac{\sinh^2\psi_w\cosh^2\psi_w}{\{\sinh^2\psi_w + \sin^2[\pi(t+s)/2]\}^2} \\ \mathcal{B}(t,s) &= \frac{\frac{1}{2}\cosh(2\psi_w)}{\sinh^2\psi_w + \sin^2[\pi(t+s)/2]} \end{aligned} \tag{96}$$

Elliptical Annular Wing with $b_w < a_w$

Equation (92) is used. The coefficient of lift is given in Eq. (93). The coefficient of induced drag is

$$C_{D_i} = -\frac{\pi}{16b_w l V_\infty^4}\int_{-1}^{+1} m(s)\int_{-1}^{+1} m(t)[\bar{\mathcal{A}}(t,s) - \bar{\mathcal{B}}(t,s)]\,\mathrm{d}t\,\mathrm{d}s - \frac{\pi}{16b_w l V_\infty^4}\int_{-1}^{+1} m(s)\,\Xint=_{-1}^{+1} \frac{m(t)}{1-\cos[\pi(t-s)]}\,\mathrm{d}t\,\mathrm{d}s \tag{97}$$

where

$$\begin{aligned} \bar{\mathcal{A}}(t,s) &= \frac{\sinh^2\psi_w\cosh^2\psi_w}{\{\sinh^2\psi_w + \cos^2[\pi(t+s)/2]\}^2} \\ \bar{\mathcal{B}}(t,s) &= \frac{\frac{1}{2}\cosh(2\psi_w)}{\sinh^2\psi_w + \cos^2[\pi(t+s)/2]} \end{aligned} \tag{98}$$

Convex Arcs Obtained from a Circular Annular Wing

Using the transformation

$$\varphi_d = \frac{3}{2}\pi + \varepsilon\pi t \qquad \varphi = \frac{3}{2}\pi + \varepsilon\pi s \tag{99}$$

the coefficients of lift and induced drag become

$$C_L = -\frac{2\varepsilon\pi R_w}{SV_\infty^2}\int_{-1}^{+1} m(t)\cos(\varepsilon\pi t)\,\mathrm{d}t \tag{100}$$

$$C_{D_i} = -\frac{\varepsilon^2\pi}{4SV_\infty^4}\int_{-1}^{+1} m(s)\left(\oint_{-1}^{+1}\frac{m(t)}{1-\cos[\varepsilon\pi(t-s)]}\,\mathrm{d}t\right)\mathrm{d}s \quad (101)$$

Concave Arcs Obtained from a Circular Annular Wing

Using the transformation

$$\varphi_d = \frac{\pi}{2} + \varepsilon\pi t \qquad \varphi = \frac{\pi}{2} + \varepsilon\pi s \quad (102)$$

$$C_L = +\frac{2\varepsilon\pi R_w}{SV_\infty^2}\int_{-1}^{+1} m(t)\cos(\varepsilon\pi t)\,\mathrm{d}t \quad (103)$$

$$C_{D_i} = -\frac{\varepsilon^2\pi}{4SV_\infty^4}\int_{-1}^{+1} m(s)\left(\oint_{-1}^{+1}\frac{m(t)}{1-\cos[\varepsilon\pi(t-s)]}\,\mathrm{d}t\right)\mathrm{d}s \quad (104)$$

Note that the expression of the coefficient of induced drag is formally the same as Eq. (101).

Convex Arcs Obtained from an Elliptical Annular Wing with $b_w > a_w$

Using the transformation (99)

$$C_L = -\frac{2\varepsilon\pi b_w}{SV_\infty^2}\int_{-1}^{+1} m(t)\cos(\varepsilon\pi t)\,\mathrm{d}t \quad (105)$$

$$C_{D_i} = -\frac{\varepsilon^2\pi}{4SV_\infty^4}\int_{-1}^{+1} m(s)\int_{-1}^{+1} m(t)[\mathcal{C}(t,s,\varepsilon) - \mathcal{D}(t,s,\varepsilon)]\,\mathrm{d}t\,\mathrm{d}s - \frac{\varepsilon^2\pi}{4SV_\infty^4}\int_{-1}^{+1} m(s)\oint_{-1}^{+1}\frac{m(t)}{1-\cos[\varepsilon\pi(t-s)]}\,\mathrm{d}t\,\mathrm{d}s \quad (106)$$

where

$$\mathcal{C}(t,s,\varepsilon) = \frac{\sinh^2\psi_w\cosh^2\psi_w}{\{\sinh^2\psi_w + \cos^2[\varepsilon\pi(t+s)/2]\}^2}$$
$$\mathcal{D}(t,s,\varepsilon) = \frac{\frac{1}{2}\cosh(2\psi_w)}{\sinh^2\psi_w + \cos^2[\varepsilon\pi(t+s)/2]} \quad (107)$$

Concave Arcs Obtained from an Elliptical Annular Wing with $b_w > a_w$

The transformation used is reported in Eq. (102). The expression of the coefficient of induced drag is formally identical to Eq. (106). The expression of the coefficient of lift is formally identical to Eq. (105); the only difference in this case is the sign (which is positive).

Convex Arcs Obtained from an Elliptical Annular Wing with $b_w < a_w$

Using the transformation (99) it is possible to demonstrate that the coefficient of lift is represented by Eq. (105). The coefficient of induced drag is

$$C_{D_i} = -\frac{\varepsilon^2\pi}{4SV_\infty^4}\int_{-1}^{+1} m(s)\int_{-1}^{+1} m(t)[\bar{\mathcal{C}}(t,s,\varepsilon) - \bar{\mathcal{D}}(t,s,\varepsilon)]\,\mathrm{d}t\,\mathrm{d}s - \frac{\varepsilon^2\pi}{4SV_\infty^4}\int_{-1}^{+1} m(s)\oint_{-1}^{+1}\frac{m(t)}{1-\cos[\varepsilon\pi(t-s)]}\,\mathrm{d}t\,\mathrm{d}s \quad (108)$$

where

$$\bar{\mathcal{C}}(t,s,\varepsilon) = \frac{\sinh^2\psi_w\cosh^2\psi_w}{\{\sinh^2\psi_w + \sin^2[\varepsilon\pi(t+s)/2]\}^2}$$
$$\bar{\mathcal{D}}(t,s,\varepsilon) = \frac{\frac{1}{2}\cosh(2\psi_w)}{\sinh^2\psi_w + \sin^2[\varepsilon\pi(t+s)/2]} \quad (109)$$

Concave Arcs Obtained from an Elliptical Annular Wing with $b_w < a_w$

Using Eq. (102), it is possible to show that the expression of the coefficient of lift is formally identical to Eq. (105); the only difference in this case is the sign (which is positive). The coefficient of induced drag is formally identical to Eq. (108).

Annular Wings: Minimum Induced Drag

Circular Annular Wing

To find the doublet distribution corresponding to the minimum induced drag when the wing span is fixed and the coefficient of lift is fixed (for example, $C_L = \bar{C}_L$), the expressions (93) and (94), and the Euler–Lagrange Eq. (17) have to be used. Before these operations, it should be noticed that the circular wing does not have a unique optimal solution because the wing is a closed wing system (this will be demonstrated later). Thus, if m_{opt} is a solution for the minimization problem, the distribution $m'_{\text{opt}} = m_{\text{opt}} + \text{const}$ is a solution too. In the particular case in which const $= 0$, the optimal distribution is called *fundamental distribution*. The definition of the fundamental distribution is then an arbitrary quantity. Considering the symmetry of the wing system, the optimal fundamental doublet distribution m_{opt} is chosen to be the one that is zero at the points $y = \pm b_w$. With this choice, the fundamental distribution will be zero in *both* the limits of the integrals ($\varphi = 0$ and $\varphi = 2\pi$ or $t = -1$ and $t = +1$). This justifies the assumption earlier adopted [$m(0) = m(2\pi) = 0$] in the expression of the induced drag.

In the case of circular wing the following relations are valid:

$$C_1 = -\frac{\pi}{16R_w l V_\infty^4} \qquad C_2 = -\frac{\pi}{2V_\infty^2 l} \qquad g_2 = \sin(\pi t)$$
$$^R\bar{Y}(t,s) = 0 \qquad ^S\bar{Y}(t,s) = \frac{1}{1-\cos[\pi(t-s)]} \qquad \bar{C} = \bar{C}_L \quad (110)$$

The system represented by the Euler–Lagrange equation (Eq. (17)) and the constraint $C_L = \bar{C}_L$ will be

$$\begin{cases} \dfrac{1}{4R_w V_\infty^2}\oint_{-1}^{+1}\dfrac{m_{\text{opt}}(s)}{1-\cos[\pi(t-s)]}\,\mathrm{d}s - \lambda\sin(\pi t) = 0 \\ \bar{C}_L = -\dfrac{\pi}{2V_\infty^2 l}\displaystyle\int_{-1}^{+1} m_{\text{opt}}(t)\sin(\pi t)\,\mathrm{d}t \end{cases} \quad (111)$$

Analytical Solution of the Euler–Lagrange Equation

Examination of the system of Eqs. (111) shows that the function $\sin(\pi t)$ appears explicitly in both equations. This function is a continuous and periodical function, as it has to be for m_{opt}. The function is zero when $t = \pm 1$ and $t = 0$ (which correspond to $y = \pm b_w$), as is expected. Therefore, the aim is to verify whether this function satisfies the system (111). The following expression of the optimal distribution is assumed:

$$m_{\text{opt}}(t) = k\sin(\pi t) \qquad k \text{ real number} \quad (112)$$

In Appendix B it is shown that under the assumption (112) the integral is

$$\oint_{-1}^{+1}\frac{m_{\text{opt}}(s)}{1-\cos[\pi(t-s)]}\,\mathrm{d}s = -2k\sin(\pi t) \quad (113)$$

Substitution into Eq. (111) shows that it is satisfied. From the equation representing the constraint, the value of k can be found. Thus, the optimal distribution is

$$m_{\text{opt}}(t) = -\frac{2lV_\infty^2\bar{C}_L}{\pi}\sin(\pi t) \quad (114)$$

and the Lagrange multiplier is

$$\lambda = \frac{l\bar{C}_L}{\pi R_w} \quad (115)$$

The normalwash under optimal conditions is

$$(u_n)_{\text{opt}}(t) = \frac{1}{8V_\infty R_w} \fint_{-1}^{+1} \frac{m_{\text{opt}}(s)}{1-\cos[\pi(t-s)]}\,\mathrm{d}s$$
$$= \frac{1}{8V_\infty R_w}\left[\frac{4lV_\infty^2 \bar{C}_L}{\pi}\sin(\pi t)\right] = \frac{lV_\infty \bar{C}_L}{2\pi R_w}\sin(\pi t) \qquad (116)$$

In the original variables (it is not important if φ or φ_d is used) the final expressions of the fundamental optimal doublet distribution and of the normalwash are

$$m_{\text{opt}}(\varphi) = \frac{2lV_\infty^2 \bar{C}_L}{\pi}\sin\varphi \qquad (u_n)_{\text{opt}}(\varphi) = -\frac{lV_\infty \bar{C}_L}{2\pi R_w}\sin\varphi \quad (117)$$

The coefficient of minimum induced drag is (the subscript $b_w/a_w = 1$ is used to underline that the coefficient is referred to the circular annular wing, where $a_w = b_w = R_w$)

$$[(C_{D_i})_{\text{opt}}]_{b_w/a_w=1} = \frac{l\bar{C}_L^2}{2\pi R_w} \qquad (118)$$

To compare the wing performance with a classical wing, it is better to calculate the *minimum* induced drag and efficiency from the definitions of coefficients of induced drag and lift:

$$[(D_i)_{\text{opt}}]_{b_w/a_w=1} = \frac{\bar{L}^2}{2\pi q(2R_w)^2} \qquad [(E)_{\text{opt}}]_{b_w/a_w=1} = \frac{2\pi q(2R_w)^2}{\bar{L}} \qquad (119)$$

where $q = \frac{1}{2}\rho_\infty V_\infty^2$. Now consider a classical cantilevered wing with *the same total lifting force* and the same wing span $2b_w$ (notice that for circular wing $b_w = R_w$). The efficiency under *optimal condition* is calculated using an elliptical distribution:

$$[(E)_{\text{opt}}]_{\text{ref}} = \frac{\pi q(2b_w)^2}{\bar{L}} \qquad (120)$$

Hence, using (119), it is deduced that

$$\frac{[(E)_{\text{opt}}]_{b_w/a_w=1}}{[(E)_{\text{opt}}]_{\text{ref}}} = 2 \qquad (121)$$

This last result shows the great aerodynamic advantage of the closed-wing system. It is also in perfect accord with the known value found by Cone [19].

The Euler–Lagrange equation can be solved numerically [6]. This last calculation has been performed [14] and it has shown excellent correlation with the analytical values reported here.

According to the notation reported in Appendix C of [6], the numerical analysis has been performed using $N = 20$ collocation points. $M = 200$ nodes were used in the quadrature formulas for the Hadamard integrals {see Eq. (C2) of [6]}.

Verification of Munk's Minimum Induced Drag Theorem

Munk's [20] minimum induced drag theorem states:

> When all the elements of a lifting system have been translated into a single plane (Munk's stagger theorem), the induced drag will be minimum when the component of the induced velocity normal to the lifting element at each point is proportional to the cosine of the angle of inclination of the lifting element at that point.

This theorem is explained graphically in Fig. 10. If the doublet distribution m_{opt} [Eq. (117)] is effectively the fundamental optimal distribution, Munk's minimum induced drag theorem has to be satisfied (see Fig. 11). Thus

$$\frac{(u_n)_{\text{opt}}}{\cos\vartheta} = \frac{-(lV_\infty \bar{C}_L \sin\varphi)/(2\pi R_w)}{\sin\varphi} = -\frac{lV_\infty \bar{C}_L}{2\pi R_w} = \text{const} \qquad (122)$$

The theorem is verified.

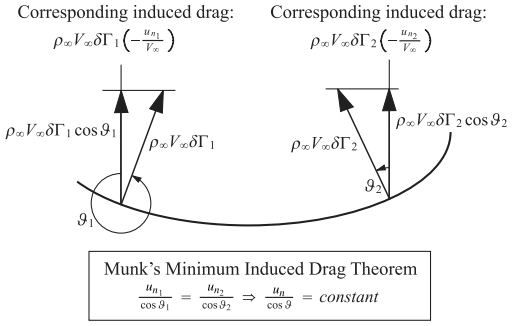

Fig. 10 Munk's minimum induced drag theorem in a nonplanar wing.

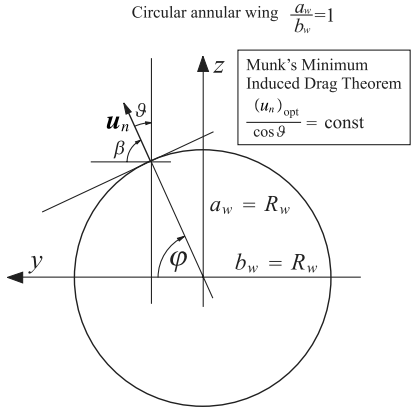

Fig. 11 Circular annular wing and Munk's minimum induced drag theorem.

Doublet Distribution of Minimum Induced Drag: Nonuniqueness of the Solution

The solution is not unique. In particular, if m_{opt} is a solution for the minimization problem, the distribution $m'_{\text{opt}} = m_{\text{opt}} + \text{const}$ is a solution too. This property can be verified for the circular wing. To demonstrate the property, it is sufficient to show that for a constant doublet distribution the lift and induced drag are zero. The first verification is very simple and is omitted here. The second property, however, will be verified.

Suppose that $m = \text{const} = \bar{m}$. If the doublet distribution is constant, then the circulation is constant and the induced drag (which depends on the gradients of the circulation) is zero. This can also be directly verified by calculating the inner integral of the induced drag coefficient (under the assumption of constant doublet distribution):

$$\fint_0^{2\pi} \frac{m(\varphi_d)}{1-\cos(\varphi_d-\varphi)}\,\mathrm{d}\varphi_d = \bar{m}\fint_0^{2\pi} \frac{1}{1-\cos(\varphi_d-\varphi)}\,\mathrm{d}\varphi_d = 0 \qquad (123)$$

The inner integral is zero and so the induced drag (which is its integral) is zero as well.

Minimum Induced Drag in an Elliptical Annular Wing with $b_w > a_w$

Most of the derivations and theoretical considerations are still valid. Therefore some details will be omitted. In the case of annular wing with $b_w > a_w$, the following relations are valid:

$$C_1 = -\frac{\pi}{16 b_w l V_\infty^4} \qquad C_2 = -\frac{\pi}{2V_\infty^2 l} \qquad g_2 = \sin(\pi t)$$
$$^R\bar{Y}(t,s) = \mathcal{A}(t,s) - \mathcal{B}(t,s) \qquad ^S\bar{Y}(t,s) = \frac{1}{1-\cos[\pi(t-s)]}$$
$$\bar{C} = \bar{C}_L \qquad (124)$$

The Euler–Lagrange equation [Eq. (17)] is in this case

$$\begin{cases} +\dfrac{1}{4b_w V_\infty^2}\displaystyle\int_{-1}^{+1} m_{\text{opt}}(s)[\mathcal{A}(t,s)-\mathcal{B}(t,s)]\,\mathrm{d}s \\ +\dfrac{1}{4b_w V_\infty^2}\displaystyle\oint_{-1}^{+1} \dfrac{m_{\text{opt}}(s)}{1-\cos[\pi(t-s)]}\,\mathrm{d}s-\lambda\sin(\pi t)=0 \\ \\ \bar{C}_L=-\dfrac{\pi}{2V_\infty^2 l}\displaystyle\int_{-1}^{+1} m_{\text{opt}}(t)\sin(\pi t)\,\mathrm{d}t \end{cases} \tag{125}$$

Analytical Solution of the Euler–Lagrange Equation

Equation (125) is quite similar to Eq. (111) valid for the circular annular wing. Therefore, a solution in the form (112) is sought. Equation (125) can be written in a more concise form as

$$\begin{cases} +\dfrac{1}{4b_w V_\infty^2} I_A-\dfrac{1}{4b_w V_\infty^2} I_B+\dfrac{1}{4b_w V_\infty^2} I_C-\lambda\sin(\pi t)=0 \\ \bar{C}_L=-\dfrac{\pi}{2V_\infty^2 l}\displaystyle\int_{-1}^{+1} m_{\text{opt}}(t)\sin(\pi t)\,\mathrm{d}t \end{cases} \tag{126}$$

The Hadamard integral is calculated in Appendix A: $I_C = -2k\sin(\pi t)$. The regular integrals do not show particular problems. It can be shown that

$$\begin{aligned} I_A &= -2k\frac{\sin(\pi t)}{\sinh 2\psi_w} \\ I_B &= 2k\sin(\pi t)\cosh(2\psi_w)\left(1-\frac{\cosh 2\psi_w}{\sinh 2\psi_w}\right) \end{aligned} \tag{127}$$

Substituting I_A, I_B, I_C in the system (126)

$$\begin{cases} \lambda=\dfrac{l\bar{C}_L}{\pi b_w}(\cosh 2\psi_w-\sinh 2\psi_w+1) \\ k=-\dfrac{2lV_\infty^2}{\pi}\bar{C}_L \end{cases} \tag{128}$$

using the relations

$$\begin{aligned} \cosh 2\psi_w &= 2\cosh^2\psi_w-1=2\frac{b_w^2}{b_w^2-a_w^2}-1=\frac{b_w^2+a_w^2}{b_w^2-a_w^2} \\ \sinh 2\psi_w &= 2\cosh\psi_w\sinh\psi_w=2\frac{b_w}{\sqrt{b_w^2-a_w^2}}\frac{a_w}{\sqrt{b_w^2-a_w^2}} \\ &= 2\frac{a_w b_w}{b_w^2-a_w^2} \end{aligned} \tag{129}$$

the Lagrange multiplier becomes

$$\lambda=\frac{2l\bar{C}_L}{\pi(b_w+a_w)} \tag{130}$$

Notice that, if $b_w \to a_w = R_w$ (circular annular wing), $\lambda = (l\bar{C}_L)/(\pi R_w)$, as has been found for the circular annular wing. Consider the normalwash [Eq. (56)]. Changing the variables in t, s and using the expressions for the integrals I_A, I_B, and I_C, it can be obtained the normalwash under optimal conditions (notice that when $b_w \to a_w = R_w$ the normalwash of the circular wing under optimal conditions is obtained):

$$(u_n)_{\text{opt}}=-\frac{\sin\varphi\cosh\psi_w}{h_{w\varphi}}\frac{lV_\infty\bar{C}_L(\cosh\psi_w-\sinh\psi_w)}{c\pi} \tag{131}$$

In Fig. 12, the *optimal fundamental doublet distribution* is shown for a particular case. Using the quantities I_A, I_B, and I_C the coefficient of minimum induced drag can be calculated:

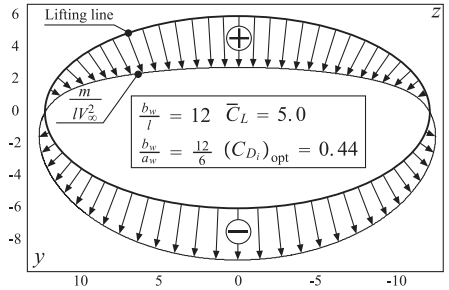

Fig. 12 Elliptical annular wing with $b_w > a_w$. Doublet distribution under optimal conditions.

$$[(C_{D_i})_{\text{opt}}]_{b_w/a_w>1}=\frac{l\bar{C}_L^2}{\pi(b_w+a_w)} \tag{132}$$

and the corresponding induced drag is

$$[(D_i)_{\text{opt}}]_{b_w/a_w>1}=\frac{\bar{L}^2}{\pi q(1+a_w/b_w)(2b_w)^2} \tag{133}$$

The optimal aerodynamic efficiency is

$$[(E)_{\text{opt}}]_{b_w/a_w>1}=\frac{\pi q(1+a_w/b_w)(2b_w)^2}{\bar{L}} \tag{134}$$

Using the expression of the efficiency in a classical cantilevered wing with *the same total lifting force* and the same wing span $2b_w$,

$$\frac{[(E)_{\text{opt}}]_{b_w/a_w>1}}{[(E)_{\text{opt}}]_{\text{ref}}}=1+\frac{a_w}{b_w} \tag{135}$$

From the preceding equation, it is clear that $1 < [(E)_{\text{opt}}]_{b_w/a_w>1}/[(E)_{\text{opt}}]_{\text{ref}} < 2$. It is also clear that

$$\lim_{a_w\to 0}\frac{[(E)_{\text{opt}}]_{b_w/a_w>1}}{[(E)_{\text{opt}}]_{\text{ref}}}=1 \tag{136}$$

$$\lim_{a_w\to b_w}\frac{[(E)_{\text{opt}}]_{b_w/a_w>1}}{[(E)_{\text{opt}}]_{\text{ref}}}=2 \tag{137}$$

The elliptical annular wing with $b_w > a_w$ has the same induced drag (under optimal condition) as a cantilevered classical wing when $a_w \to 0$. Moreover, the elliptical annular wing with $b_w > a_w$ has the same induced drag (under optimal condition) as a circular annular wing when $a_w \to b_w$. This is in perfect accord with the results obtained by Cone [19]. The numerical solution of the Euler–Lagrange equation confirmed these theoretical predictions.

Verification of Munk's Minimum Induced Drag Theorem

In this case it can be seen that

$$\cos\vartheta=\sin\beta=\frac{\cosh\psi_w\sin\varphi}{h_{w\varphi}} \tag{138}$$

Using this expression, Munk's minimum induced drag theorem can be shown to be satisfied:

$$\begin{aligned} &\frac{(u_n)_{\text{opt}}}{\cos\vartheta} \\ &\quad=\frac{-[(\cosh\psi_w\sin\varphi)/h_{w\varphi}]\{[lV_\infty\bar{C}_L(\cosh\psi_w-\sinh\psi_w)]/(\pi c)\}}{(\cosh\psi_w\sin\varphi)/h_{w\varphi}} \\ &\quad=-\frac{lV_\infty\bar{C}_L(\cosh\psi_w-\sinh\psi_w)}{\pi c}=\text{const} \end{aligned} \tag{139}$$

Doublet Distribution of Minimum Induced Drag: Nonuniqueness of the Solution

As for the circular wing, it is sufficient to prove that the coefficient of lift and induced drag for a distribution $m = \text{const} = \bar{m}$ is zero. This is clear if it is considered again that the induced drag depends on the gradient of the circulation. Mathematically it can be shown as follows. The Hadamard integral of the induced-drag expression is formally identical to the one found for the circular annular wing. Therefore, if $m = \text{const} = \bar{m}$ then the Hadamard integral is zero [see Eq. (123)]. The part of the induced-drag coefficient which contains only regular integrals is

$$C_{D_i}^{\text{reg}} = -\frac{\bar{m}^2\pi}{16 b_w l V_\infty^4}\int_{-1}^{+1}(I'_A - I'_B)\,\mathrm{d}s \tag{140}$$

where

$$\begin{aligned} I'_A &= \int_{-1}^{+1}\mathcal{A}(t,s)\,\mathrm{d}t = \frac{\cosh(2\psi_w)}{\sinh\psi_w\cosh\psi_w} \\ I'_B &= \int_{-1}^{+1}\mathcal{B}(t,s)\,\mathrm{d}t = \frac{\cosh(2\psi_w)}{\sinh\psi_w\cosh\psi_w} = I'_A \end{aligned} \tag{141}$$

Therefore, $C_{D_i} = 0$. Thus, the property is demonstrated.

Minimum Induced Drag in an Elliptical Annular Wing with $b_w < a_w$

The derivation of the Euler–Lagrange is straightforward and is omitted here. For details it is sufficient to refer to the elliptical annular wing in which $b_w > a_w$. It is possible to show that

$$\lambda = \frac{2l\bar{C}_L}{\pi(b_w + a_w)} \tag{142}$$

$$m_{\text{opt}}(\varphi) = \frac{2lV_\infty^2\bar{C}_L}{\pi}\sin(\varphi) \tag{143}$$

$$(u_n)_{\text{opt}} = -\frac{\sin\varphi\sinh\psi_w}{\bar{h}_{w\varphi}}\frac{lV_\infty\bar{C}_L(\cosh\psi_w - \sinh\psi_w)}{c\pi} \tag{144}$$

The coefficient of minimum induced drag is

$$[(C_{D_i})_{\text{opt}}]_{b_w/a_w<1} = \frac{l\bar{C}_L^2}{\pi(b_w + a_w)} \tag{145}$$

The corresponding induced drag is

$$[(D_i)_{\text{opt}}]_{b_w/a_w<1} = \frac{\bar{L}^2}{\pi q(1 + a_w/b_w)(2b_w)^2} \tag{146}$$

whereas the aerodynamic efficiency is

$$[(E)_{\text{opt}}]_{b_w/a_w<1} = \frac{\pi q(1 + a_w/b_w)(2b_w)^2}{\bar{L}} \tag{147}$$

Using the expression of efficiency in a classical cantilevered wing with *the same total lifting force* and the same wing span $2b_w$,

$$\frac{[(E)_{\text{opt}}]_{b_w/a_w<1}}{[(E)_{\text{opt}}]_{\text{ref}}} = 1 + \frac{a_w}{b_w} \tag{148}$$

In the preceding equation, notice that $2 < [(E)_{\text{opt}}]_{b_w/a_w<1}/[(E)_{\text{opt}}]_{\text{ref}} < \infty$. It is also clear that

$$\lim_{a_w\to b_w}\frac{[(E)_{\text{opt}}]_{b_w/a_w<1}}{[(E)_{\text{opt}}]_{\text{ref}}} = 2 \tag{149}$$

$$\lim_{a_w\to\infty}\frac{[(E)_{\text{opt}}]_{b_w/a_w<1}}{[(E)_{\text{opt}}]_{\text{ref}}} = \infty \tag{150}$$

The elliptical annular wing with $b_w < a_w$ has the same induced drag (under optimal condition) as a circular wing when $a_w \to b_w$. Moreover, the elliptical annular wing with $b_w < a_w$ has infinite efficiency when $a_w \to \infty$.

But this does not mean that, effectively, this condition can be reached, because other aspects of the problem should be considered. For example, the weight of the wing was not taken into account. If it were, then, clearly, the condition $a_w \to \infty$ would imply infinite weight and this is not acceptable. However, these analyses show that the aerodynamic of the closed-wing system is very good.

Verification of Munk's Minimum Induced Drag Theorem

If the doublet distribution m_{opt} is effectively the fundamental optimum distribution, Munk's minimum induced drag theorem has to be satisfied. Using the relation

$$\cos\vartheta = \sin\beta = \frac{\sinh\psi_w\sin\varphi}{\bar{h}_{w\varphi}} \tag{151}$$

it is easy to verify that the theorem is satisfied:

$$\begin{aligned} &\frac{(u_n)_{\text{opt}}}{\cos\vartheta} \\ &\quad= \frac{-[(\sinh\psi_w\sin\varphi)/\bar{h}_{w\varphi}]\{[lV_\infty\bar{C}_L(\cosh\psi_w - \sinh\psi_w)]/(\pi c)\}}{(\sinh\psi_w\sin\varphi)/\bar{h}_{w\varphi}} \\ &\quad= -\frac{lV_\infty\bar{C}_L(\cosh\psi_w - \sinh\psi_w)}{\pi c} = \text{const} \end{aligned} \tag{152}$$

The nonuniqueness of the solution can be demonstrated using the same procedure shown for the case in which $b_w > a_w$. This demonstration is omitted here because it does not add new information.

Annular Wings and Classical Wings: Comparison

The obtained results are summarized in this section. The ratio between the aerodynamic efficiency of the annular wings and the efficiency of the classical cantilevered wings is reported in Fig. 13.

Elliptical Annular Wing and Biplane: Comparison

Following the same procedure, the conditions that guarantee the minimum induced drag can be found, also, for the biplane [6]. But it is interesting to understand when an elliptical annular wing will be better than a biplane (both under the condition of minimum induced drag). First of all, it must be decided which is the best ellipse to compare with the biplane. Considering the fact that the ellipse has curved extremities, a biplane with the distance between the wings equal to H can be compared with an elliptical annular wing with $a_w = H$ (this is not the only possible choice). The optimal induced-drag coefficient is compared in Fig. 14. The reference surface in both cases and in the cantilevered wing (the reference value) is the same: $S = 4b_w l$. From Fig. 14, it is clear that, *for small aspect ratio, the annular wing and biplane show similar behavior*, whereas for high aspect ratio the tendency is the opposite (the biplane has a minimum value of induced drag equal to half the induced-drag of a classical wing when the wings are indefinitely distant, whereas an elliptical annular wing does not have this limit).

Elliptical Lifting Arcs: Minimum Induced Drag

In this section, the condition corresponding to the minimum induced drag will be studied, as was done for the annular wings and the biplane [6]. The results will be compared with the classical cantilevered wing and with the corresponding annular wing and with the literature [19]. The most advantageous point to close the wing is found and the differences between annular wings and C-wings [3] understood. Kroo's results will be confirmed: the C-wings have similar induced drag to that of the closed wing systems. The purpose

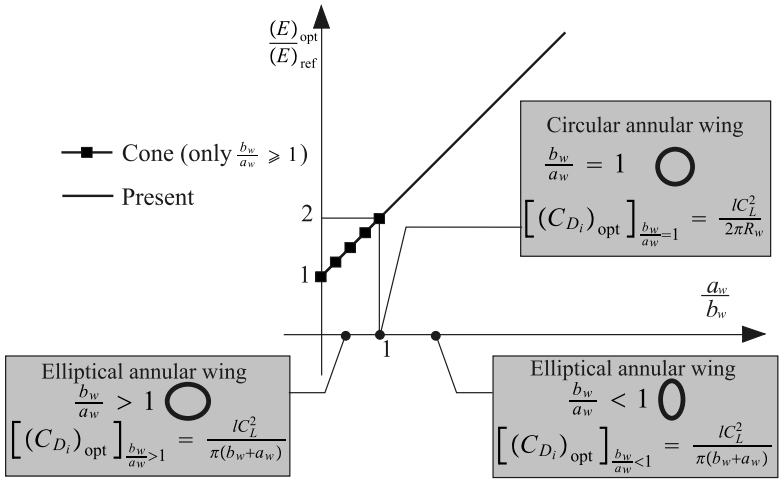

Fig. 13 Efficiency of the annular wings. Comparison with Cone's [19] results.

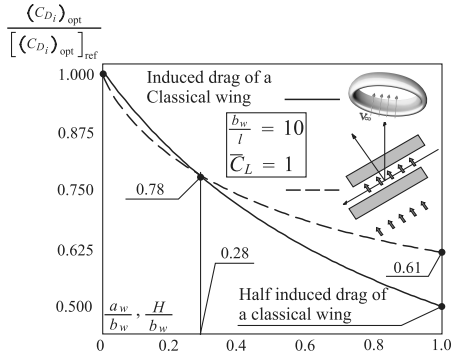

Fig. 14 Biplane and elliptical annular wing under optimal conditions.

of the present analyses is to demonstrate that this formulation is a good tool for the preliminary study of new configurations.

Minimum Induced Drag in a Convex Elliptical Lifting Arc

Only the case in which $b_w > a_w$ is analyzed in detail. The others are similar. Consider Eqs. (105), (106), and (17). It appears clear that in this case the following relations are valid:

$$C_1 = -\frac{\varepsilon^2\pi}{4SV_\infty^4} \qquad C_2 = -\frac{2\varepsilon\pi b_w}{SV_\infty^2} \qquad g_2 = \cos(\varepsilon\pi t)$$

$${}^R\bar{Y}(t,s) = \mathcal{C}(t,s,\varepsilon) - \mathcal{D}(t,s,\varepsilon) \qquad {}^S\bar{Y}(t,s) = \frac{1}{1-\cos[\varepsilon\pi(t-s)]}$$

$$\bar{C} = \bar{C}_L \tag{153}$$

Therefore, the system represented by the Euler–Lagrange and the constraint is

$$\begin{cases} +\dfrac{\varepsilon}{2V_\infty^2}\displaystyle\int_{-1}^{+1} m_{\text{opt}}(s)[\mathcal{C}(t,s,\varepsilon) - \mathcal{D}(t,s,\varepsilon)]\,\mathrm{d}s \\ +\dfrac{\varepsilon}{2V_\infty^2}\displaystyle\oint_{-1}^{+1} \frac{m_{\text{opt}}(s)}{1-\cos[\varepsilon\pi(t-s)]}\,\mathrm{d}s - 2b_w\lambda\cos(\varepsilon\pi t) = 0 \\ \\ \bar{C}_L = -\dfrac{2\varepsilon\pi b_w}{S^2V_\infty^2}\displaystyle\int_{-1}^{+1} m_{\text{opt}}(t)\cos(\varepsilon\pi t)\,\mathrm{d}t \end{cases} \tag{154}$$

Minimum Induced Drag in a Concave Elliptical Lifting Arc

Only the case in which $b_w > a_w$ is analyzed in detail. The others are similar. It appears clear that in this case the following relations are valid:

$$C_1 = -\frac{\varepsilon^2\pi}{4SV_\infty^4} \qquad C_2 = +\frac{2\varepsilon\pi b_w}{SV_\infty^2} \qquad g_2 = \cos(\varepsilon\pi t)$$

$${}^R\bar{Y}(t,s) = \mathcal{C}(t,s,\varepsilon) - \mathcal{D}(t,s,\varepsilon) \qquad {}^S\bar{Y}(t,s) = \frac{1}{1-\cos[\varepsilon\pi(t-s)]}$$

$$\bar{C} = \bar{C}_L \tag{155}$$

Therefore, the system represented by the Euler–Lagrange and the constraint is

$$\begin{cases} +\dfrac{\varepsilon}{2V_\infty^2}\displaystyle\int_{-1}^{+1} m_{\text{opt}}(s)[\mathcal{C}(t,s,\varepsilon) - \mathcal{D}(t,s,\varepsilon)]\,\mathrm{d}s \\ +\dfrac{\varepsilon}{2V_\infty^2}\displaystyle\oint_{-1}^{+1} \frac{m_{\text{opt}}(s)}{1-\cos[\varepsilon\pi(t-s)]}\,\mathrm{d}s + 2b_w\lambda\cos(\varepsilon\pi t) = 0 \\ \\ \bar{C}_L = +\dfrac{2\varepsilon\pi b_w}{SV_\infty^2}\displaystyle\int_{-1}^{+1} m_{\text{opt}}(t)\cos(\varepsilon\pi t)\,\mathrm{d}t \end{cases} \tag{156}$$

Convex and Concave Elliptical Lifting Arcs: Comparison Under Optimal Conditions

Consider a convex arc and a concave arc that come from the same annular wing. Suppose also that the parameter ε is the same in both the arcs. Let $[m_{\text{opt}}]_{\text{convex}}$ be the optimal distribution of the convex arc. By definition, $[m_{\text{opt}}]_{\text{convex}}$ satisfies both equations of the system (154).

Now, focus on the concave arc. $[m_{\text{opt}}]_{\text{concave}}$ is the *unknown* optimal doublet distribution. If it is chosen as

$$[m_{\text{opt}}]_{\text{concave}} = -[m_{\text{opt}}]_{\text{convex}} \tag{157}$$

then the constraint [second equation of the system (156)] is satisfied. In fact, the constraint of the concave arc becomes formally identical to the constraint valid for the convex arc and, by definition, $[m_{\text{opt}}]_{\text{convex}}$ satisfies this constraint. If Eq. (157) is substituted into the Euler–Lagrange equation of a concave arc [first expression of the system (156)], in a formal point of view, the Euler–Lagrange equation of a convex arc [first expression of the system (154)] is the obtained result. And this is then satisfied because, again, by definition $[m_{\text{opt}}]_{\text{convex}}$ satisfies the first relation of the system (154). Considering, also, that the expression for the coefficient of induced drag is formally identical for convex and concave arcs with the same parameter ε [see Eq. (106)] and that the coefficient of induced drag does not change if the distribution is changed in sign, it can be deduced that *the convex arc and the concave arc have the same*

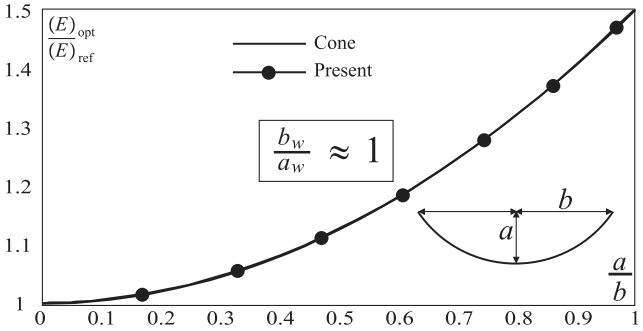

Fig. 15 Elliptical lifting arcs. Comparison with the literature [19].

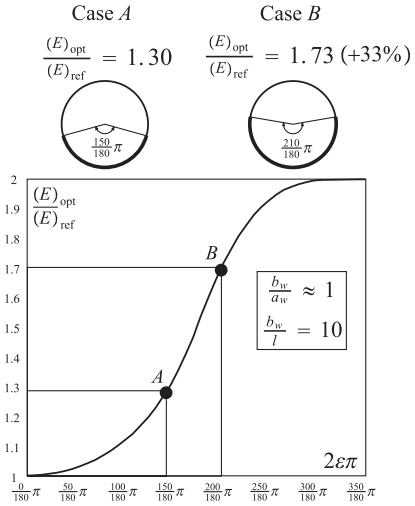

Fig. 16 Elliptical lifting arcs under optimal conditions. Comparison with a classical wing.

optimal induced drag. Considering also the positive axis direction for the doublet distribution (always toward to the local center of curvature) it appears clear that Eq. (157) states that the distribution over the arcs is the same (the sign is only a result of the positive convention chosen for the doublet distributions). The only difference between the two cases is in the *induced lift* not considered here [14,19].

Comparison Between Annular Wings and C-wings (Lifting Arcs)

First, the present method is validated using a result from Cone's paper [19]. Cone plots the efficiency ratio $(E)_{opt}/(E)_{ref}$ against the a/b ratio. As shown in Fig. 15, the present optimization procedure shows excellent correlation. In Fig. 16, the arcs with $b_w/a_w \approx 1$ are studied. In particular, the efficiency ratio with the angle $2\varepsilon\pi$ is analyzed. Clearly, when $2\varepsilon\pi \approx 0$, the curvature effects are negligible, and the efficiency is almost the same as the optimally loaded classical wing. But when the angle is increased, an increment

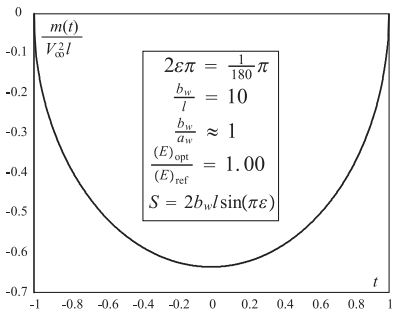

Fig. 17 Optimal doublet distribution.

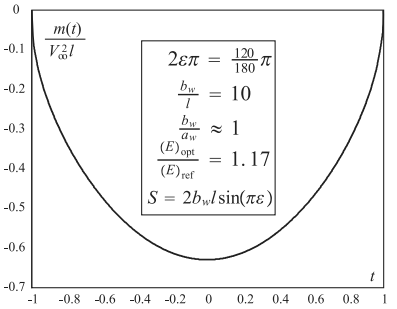

Fig. 18 Optimal doublet distribution.

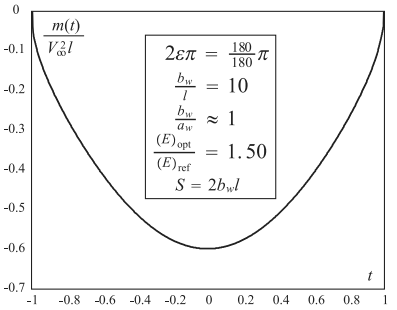

Fig. 19 Optimal doublet distribution.

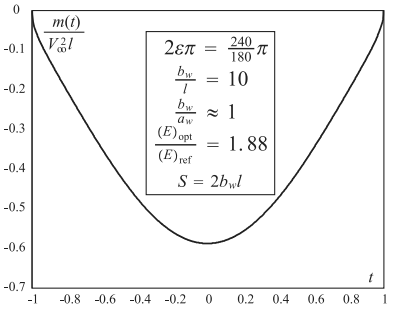

Fig. 20 Optimal doublet distribution.

of the efficiency can be observed. This is particularly evident in the range $\frac{150}{180}\pi \leq 2\varepsilon\pi \leq \frac{210}{180}\pi$, where the efficiency ratio increases by 33%. Moreover, it can be noticed that, when the arcs tend to be a closed curve, the induced drag is practically the same as the induced drag of the corresponding circular annular wing (remember that, in Fig. 16, $b_w/a_w \approx 1$). It is of interest to analyze how the optimal doublet distribution changes when the angle $2\varepsilon\pi$ is changed and what is the difference between the doublet distribution in the annular wing and the arc with $2\varepsilon\pi \approx 2\pi$ (in all cases the coefficient of lift is calculated using the reference surface given by Eq. (90); moreover, the reference efficiency is calculated using the formula relative to the classical wing with the same wing span and lift). Consider

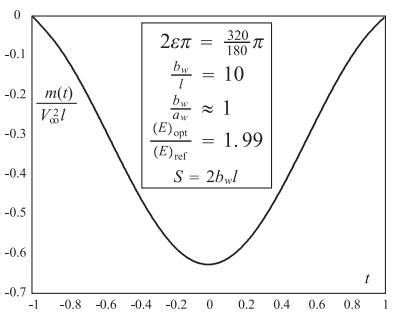

Fig. 21 Optimal doublet distribution.

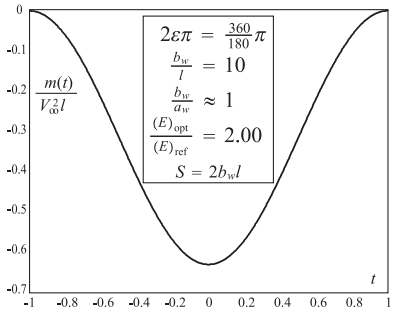

Fig. 22 Optimal doublet distribution.

Figs. 17–22. The following results can be noticed (if it is not said otherwise, consider, in all cases, $\bar{C}_L = 1$):

Result 1: The elliptical lifting arcs (and, in general, all arcs) have the same efficiency (under optimal conditions) as an optimally loaded classical wing when ε is small. Moreover, the doublet distribution is almost elliptical (see Fig. 17). This is an intuitive result: when $\varepsilon \to 0$, the curvature effects are negligible and the elliptical lifting arcs are practically a classical wing.

Result 2: When ε is not small, the efficiency increases and the doublet distribution is not an ellipse anymore. This is particularly true when the arc is almost a closed curve (see Figs. 18–22).

Result 3: When the arc is almost a closed curve (*but still an arc*) the induced drag is the same as the induced drag of the corresponding annular wing (see Fig. 22).

Result 4: The optimal doublet distribution is always different than zero, except at the tip of the wing. This is a very different situation with respect to what have been seen in the annular wings, where the fundamental distribution was sinusoidal. This property is also valid when the arc is almost a closed curve.

Figure 23 shows the nondimensional optimal doublet distribution on the lifting arcs.

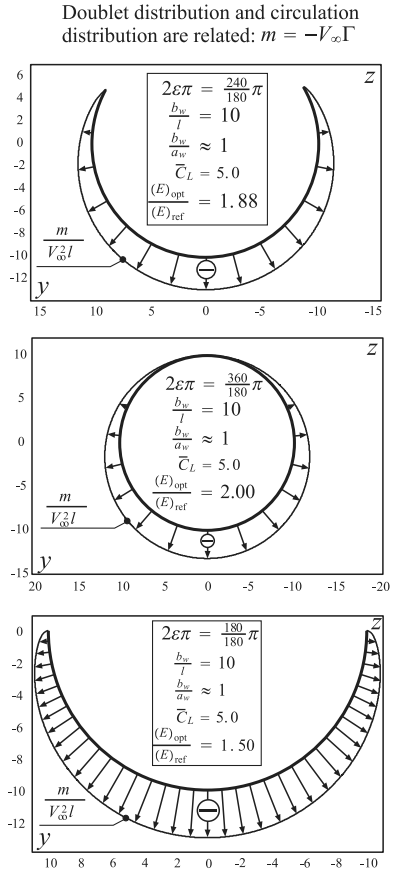

Fig. 23 Optimal doublet distribution.

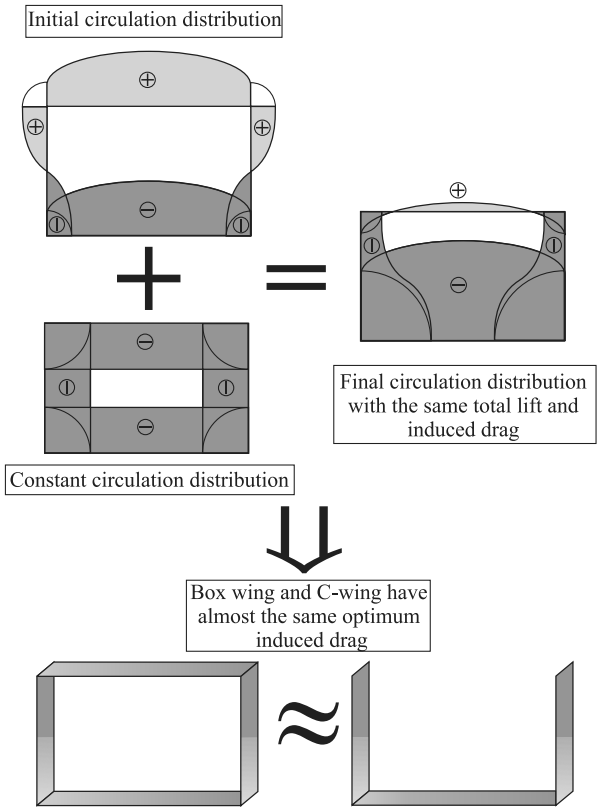

Fig. 24 Box wing and C-wing. An intuitive comparison.

The fact that the C-wing and the corresponding closed wing system have almost the same induced drag can be understood as follows: consider Fig. 24. It is possible to add a constant circulation distribution (notice that, in Fig. 24, the optimal circulation distribution in the box wing system is considered [8]) in such a way as to reduce the load in the upper wing and increase the aerodynamic load in the lower wing *without changing the total load and induced drag*. As can be seen in Fig. 24, after this ideal operation the upper wing is almost with no load which explains, in a qualitative way, the similar efficiency between the box wing and the C-wing [3]. Another important observation is that in the annular wings (and in general in the closed-wing systems) it is possible to add a constant distribution without penalty on the induced drag. As a consequence, in the closed-wing systems it is possible to change the load distribution (see Fig. 24) over the wings without penalty on the induced drag.

Extensions

The procedure presented here is general and can be used for other wing systems. Particular attention, however, has to be paid to the mathematical formulation. Suppose, for example, a nonplanar wing is to be studied and that the lifting line can be mathematically represented using n equations which represent n different curves (in the biplane $n = 2$, in the circular wing $n = 1$). The number of unknowns will be $n + 1$ (the distributions over the curves representing the wing system plus the Lagrange multiplier in the case of one constraint) and a *system* of integral equations has to be solved. Thus, the procedure shown here has to be modified and a numerical technique able to solve such systems of equations has to be introduced. Another important aspect which may introduce errors is the Hadamard integral calculation. In fact, if a wing system is (for example) made by two curves that are joined at a point, in such point the doublet distribution is in general different than zero. This complicates the formulation of the Hadamard integral: the singularity is not contained in the integration domain only, but also it can be in one (or in both) limit of the integrals. This is not a complicated problem, but different quadrature formulas have to be used.

Conclusions

Results obtained by the present procedure are in excellent correlation with the available results from the literature. It has been analytically demonstrated that closed wing systems have practically the same induced drag as the C-wings. In the closed-wing systems case it is possible to add a constant distribution without altering the total lifting force and the induced drag, whereas in the C-wing case, the distribution must be zero at the tips and, therefore, this operation cannot be done.

The procedure presented in the paper is general. It is especially practical and very useful for wing systems with only few different curves which define the integration path, such as parabolic arcs, hyperbolic arcs, sinusoidal arcs, closed-wing systems, and so forth. Once the optimal doublet distributions (in general, more than one curve is used for a wing system) are calculated, the corresponding twist distributions can be calculated using the integral equations which represent the wall tangency condition. Instead of finding the distributions m_i given the twists α_i (direct problem), the equations can be used in the inverse way: given the optimal distributions, the optimal twist can be obtained. Note that the chord is kept constant in these analyses.

Appendix A: Derivation of the Euler–Lagrange Equation

The result of the first step is

$$J = C_1 \int_{-1}^{+1} [m_{\text{opt}}(s) + \sigma\delta_1(s)] \int_{-1}^{+1} [m_{\text{opt}}(t) + \sigma\delta_1(t)]^R \bar{Y}(t,s)\,\mathrm{d}t\,\mathrm{d}s + C_1 \int_{-1}^{+1} [m_{\text{opt}}(s) + \sigma\delta_1(s)] \oint_{-1}^{+1} [m_{\text{opt}}(t) + \sigma\delta_1(t)] g_1(t,s) Y(t,s)\,\mathrm{d}t\,\mathrm{d}s \tag{A1}$$

From this expression, the derivative with respect to σ can be calculated:

$$\frac{\mathrm{d}J}{\mathrm{d}\sigma} = C_1 \int_{-1}^{+1} \delta_1(s) \int_{-1}^{+1} [m_{\text{opt}}(t) + \sigma\delta_1(t)]^R \bar{Y}(t,s)\,\mathrm{d}t\,\mathrm{d}s + C_1 \int_{-1}^{+1} [m_{\text{opt}}(s) + \sigma\delta_1(s)] \int_{-1}^{+1} \delta_1(t)^R \bar{Y}(t,s)\,\mathrm{d}t\,\mathrm{d}s + C_1 \int_{-1}^{+1} \delta_1(s) \oint_{-1}^{+1} [m_{\text{opt}}(t) + \sigma\delta_1(t)] g_1(t,s) Y(t,s)\,\mathrm{d}t\,\mathrm{d}s + C_1 \int_{-1}^{+1} [m_{\text{opt}}(s) + \sigma\delta_1(s)] \oint_{-1}^{+1} \delta_1(t) g_1(t,s) Y(t,s)\,\mathrm{d}t\,\mathrm{d}s \tag{A2}$$

The derivative, calculated for $\sigma = 0$, is

$$\left[\frac{\mathrm{d}J}{\mathrm{d}\sigma}\right]_{\sigma=0} = C_1 \int_{-1}^{+1} \delta_1(s) \int_{-1}^{+1} m_{\text{opt}}(t)^R \bar{Y}(t,s)\,\mathrm{d}t\,\mathrm{d}s + C_1 \int_{-1}^{+1} m_{\text{opt}}(s) \int_{-1}^{+1} \delta_1(t)^R \bar{Y}(t,s)\,\mathrm{d}t\,\mathrm{d}s + C_1 \int_{-1}^{+1} \delta_1(s) \oint_{-1}^{+1} m_{\text{opt}}(t) g_1(t,s) Y(t,s)\,\mathrm{d}t\,\mathrm{d}s + C_1 \int_{-1}^{+1} m_{\text{opt}}(s) \oint_{-1}^{+1} \delta_1(t) g_1(t,s) Y(t,s)\,\mathrm{d}t\,\mathrm{d}s \tag{A3}$$

The first two double integrals in Eq. (A3) are equal to each other. To prove that, it is sufficient to take the first double integral, formally switch t and s, use the symmetry of the function ${}^R\bar{Y}(t,s)$, and exchange the order of integration. After these operations, the second double integral is obtained. The last two double integrals (which contain the Hadamard integral) are equal to each other. The demonstration is the same as the demonstration valid for the first two double integrals except the fact that the exchanging order of integration is not a correct procedure a priori and it has to be proved for the Hadamard integrals [14]. Here this proof is omitted because it is not essential. After all these manipulations Eq. (A3) becomes

$$\left[\frac{\mathrm{d}J}{\mathrm{d}\sigma}\right]_{\sigma=0} = 2C_1 \int_{-1}^{+1} \delta_1(t) \int_{-1}^{+1} m_{\text{opt}}(s)^R \bar{Y}(t,s)\,\mathrm{d}s\,\mathrm{d}t + 2C_1 \int_{-1}^{+1} \delta_1(t) \oint_{-1}^{+1} m_{\text{opt}}(s) g_1(t,s) Y(t,s)\,\mathrm{d}s\,\mathrm{d}t \tag{A4}$$

Now, calculating the derivative for the constraint written in Eq. (15), it is possible to write

$$\left\{\frac{\mathrm{d}}{\mathrm{d}\sigma}\{[c_{\text{opt}}(t) + \sigma\delta_2(t)]' - C_2[m(t) + \sigma\delta_1(t)] g_2(t)\}\right\}_{\sigma=0} = \delta_2'(t) - C_2\delta_1(t) g_2(t) = 0 \tag{A5}$$

Multiplying this expression by $\lambda(t)$, integrating by parts the term which contains the derivative of δ_2 [$\delta_2(+1) = \delta_2(-1) = 0$], and adding the result to Eq. (A4), the resulting expression is

$$+ 2C_1 \int_{-1}^{+1} \delta_1(t) \int_{-1}^{+1} m_{\text{opt}}(s)^R \bar{Y}(t,s)\,\mathrm{d}s\,\mathrm{d}t + 2C_1 \int_{-1}^{+1} \delta_1(t) \oint_{-1}^{+1} m_{\text{opt}}(s) g_1(t,s) Y(t,s)\,\mathrm{d}s\,\mathrm{d}t - \int_{-1}^{+1} \lambda'(t)\delta_2(t)\,\mathrm{d}t - C_2 \int_{-1}^{+1} \lambda(t)\delta_1(t) g_2(t)\,\mathrm{d}t = 0 \tag{A6}$$

Observing that $\delta_1(t)$ and $\delta_2(t)$ are independent and arbitrary functions, $\delta_1 \equiv 0$ and $\delta_2 \equiv 0$ can be imposed separately. Imposing $\delta_1 \equiv 0$,

$$- \int_{-1}^{+1} \lambda'(t)\delta_2(t)\,\mathrm{d}t = 0 \tag{A7}$$

Because $\delta_2(t)$ is an arbitrary function, to always satisfy the previous relation, the following condition is required:

$$\lambda'(t) = 0 \Rightarrow \lambda = \text{const} \tag{A8}$$

Using this result and imposing $\delta_2 \equiv 0$, from Eq. (A6), it can be deduced that

$$2C_1 \int_{-1}^{+1} \delta_1(t) \left(\int_{-1}^{+1} m_{\text{opt}}(s)^R \bar{Y}(t,s)\,\mathrm{d}s + \oint_{-1}^{+1} m_{\text{opt}}(s) g_1(t,s) Y(t,s)\,\mathrm{d}s \right) \mathrm{d}t - C_2\lambda \int_{-1}^{+1} \delta_1(t) g_2(t)\,\mathrm{d}t = 0 \tag{A9}$$

The preceding equation can be rewritten as

$$\int_{-1}^{+1} \delta_1(t) \left(2C_1 \int_{-1}^{+1} m_{\text{opt}}(s)^R \bar{Y}(t,s)\,\mathrm{d}s + 2C_1 \oint_{-1}^{+1} m_{\text{opt}}(s) g_1(t,s) Y(t,s)\,\mathrm{d}s - C_2\lambda g_2(t) \right) \mathrm{d}t = 0 \tag{A10}$$

Again, the function $\delta_1(t)$ is arbitrary. Therefore, to satisfy Eq. (A10) the following relation has to be valid:

$$2C_1 \int_{-1}^{+1} m_{\text{opt}}(s)^R \bar{Y}(t,s)\,\mathrm{d}s + 2C_1 \oint_{-1}^{+1} m_{\text{opt}}(s) g_1(t,s) Y(t,s)\,\mathrm{d}s - C_2\lambda g_2(t) = 0 \tag{A11}$$

or equivalently,

$$2C_1 \int_{-1}^{+1} m_{\text{opt}}(s)^R \bar{Y}(t,s)\,\mathrm{d}s + 2C_1 \oint_{-1}^{+1} m_{\text{opt}}(s)^R \bar{Y}(t,s)\,\mathrm{d}s - C_2\lambda g_2(t) = 0 \tag{A12}$$

Appendix B: Hadamard Integral Under Sinusoidal Doublet Distribution

The goal is to calculate the Hadamard integral

$$I_C = \oint_{-1}^{+1} \frac{m_{\text{opt}}(s)}{1-\cos[\pi(t-s)]}\,\mathrm{d}s \tag{B1}$$

under the assumption of

$$m_{\text{opt}}(t) = k\sin(\pi t) \qquad k \text{ real number} \tag{B2}$$

Notice that the expression of the doublet distribution [Eq. (B2)] is zero in both the limits of the integral. It is convenient to use the original variables φ and φ_d. Therefore, using the transformation (92) the Hadamard integral becomes

$$I_C = \frac{1}{\pi}\oint_0^{2\pi} \frac{m_{\text{opt}}(\varphi)}{1-\cos(\varphi-\varphi_d)}\,\mathrm{d}\varphi \tag{B3}$$

Equation (B2) is

$$m_{\text{opt}}(\varphi_d) = -k\sin\varphi_d \qquad k \text{ real number} \tag{B4}$$

Thus, the integral I_C can be written as

$$I_C = -\frac{k}{\pi}\oint_0^{2\pi} \frac{\sin\varphi}{1-\cos(\varphi-\varphi_d)}\,\mathrm{d}\varphi \tag{B5}$$

or

$$\begin{aligned} I_C &= -\frac{k}{\pi}\oint_0^{\pi} \frac{\sin\varphi}{1-\cos(\varphi-\varphi_d)}\,\mathrm{d}\varphi - \frac{k}{\pi}\oint_\pi^{2\pi} \frac{\sin\varphi}{1-\cos(\varphi-\varphi_d)}\,\mathrm{d}\varphi \\ &= I_{C_1} + I_{C_2} \end{aligned} \tag{B6}$$

It is convenient to change the dummy variable φ in φ' in the integral I_{C_2}:

$$I_{C_2} = -\frac{k}{\pi}\oint_\pi^{2\pi} \frac{\sin\varphi'}{1-\cos(\varphi'-\varphi_d)}\,\mathrm{d}\varphi' \tag{B7}$$

But $\sin\varphi' = -\sin(2\pi-\varphi')$, thus

$$\begin{aligned} I_{C_2} &= -\frac{k}{\pi}\oint_\pi^{2\pi} \frac{\sin\varphi'}{1-\cos(\varphi'-\varphi_d)}\,\mathrm{d}\varphi' \\ &= -\frac{k}{\pi}\oint_\pi^{2\pi} \frac{-\sin(2\pi-\varphi')}{1-\cos(\varphi'-\varphi_d)}\,\mathrm{d}\varphi' \\ &= -\frac{k}{\pi}\oint_{2\pi}^{\pi} \frac{\sin(2\pi-\varphi')}{1-\cos(\varphi'-\varphi_d)}\,\mathrm{d}\varphi' \end{aligned} \tag{B8}$$

Observing that $\sin(2\pi-\varphi')$ is zero in both the limits of the integral and that the singularity is of order 2, it is possible to change the variables [17]. Setting

$$\begin{aligned} \varphi = 2\pi-\varphi' \Rightarrow \varphi'-\varphi_d &= 2\pi-\varphi-\varphi_d \\ \Rightarrow \cos(\varphi'-\varphi_d) &= \cos(\varphi+\varphi_d) \end{aligned} \tag{B9}$$

and observing that $\mathrm{d}\varphi = -\mathrm{d}\varphi'$, the integral I_{C_2} becomes

$$I_{C_2} = +\frac{k}{\pi}\oint_0^{\pi} \frac{\sin\varphi}{1-\cos(\varphi+\varphi_d)}\,\mathrm{d}\varphi \tag{B10}$$

Using this result, the integral I_C can be written [see Eq. (B6)]

$$\begin{aligned} I_C = I_{C_1} + I_{C_2} &= -\frac{k}{\pi}\oint_0^{\pi} \frac{\sin\varphi}{1-\cos(\varphi-\varphi_d)}\,\mathrm{d}\varphi \\ &+ \frac{k}{\pi}\oint_0^{\pi} \frac{\sin\varphi}{1-\cos(\varphi+\varphi_d)}\,\mathrm{d}\varphi \end{aligned} \tag{B11}$$

Adding I_{C_1} and I_{C_2} and observing that

$$\frac{\sin\varphi}{1-\cos(\varphi-\varphi_d)} - \frac{\sin\varphi}{1-\cos(\varphi+\varphi_d)} = 2\frac{\sin\varphi_d\sin^2\varphi}{(\cos\varphi-\cos\varphi_d)^2} \tag{B12}$$

the integral I_C becomes

$$\begin{aligned} I_C &= -\frac{k}{\pi}\oint_0^{\pi} 2\frac{\sin\varphi_d\sin^2\varphi}{(\cos\varphi-\cos\varphi_d)^2}\,\mathrm{d}\varphi \\ &= -\frac{2k\sin\varphi_d}{\pi}\oint_0^{\pi} \frac{\sin^2\varphi}{(\cos\varphi-\cos\varphi_d)^2}\,\mathrm{d}\varphi = -\frac{2k\sin\varphi_d}{\pi} I_{C_3} \end{aligned} \tag{B13}$$

The integral I_{C_3} can be calculated using a known integral. To do that, it is convenient to write the integral in the following manner:

$$\begin{aligned} I_{C_3} &= \oint_0^{\pi} \frac{\sin^2\varphi}{(\cos\varphi-\cos\varphi_d)^2}\,\mathrm{d}\varphi \\ &= \oint_\pi^{0} \frac{\sin\varphi}{(\cos\varphi-\cos\varphi_d)^2}(-\sin\varphi)\,\mathrm{d}\varphi \end{aligned} \tag{B14}$$

In the domain of integration the function $\sin\varphi$ is positive. Thus $\sin\varphi = \sqrt{1-\cos^2\varphi}$. The integral I_{C_3} can then be written as

$$I_{C_3} = \oint_\pi^{0} \frac{\sqrt{1-\cos^2\varphi}}{(\cos\varphi-\cos\varphi_d)^2}(-\sin\varphi)\,\mathrm{d}\varphi \tag{B15}$$

I_{C_3} has a function in the numerator that is zero in both the limits of the integral and the singularity is of order 2. The changing of variable is allowed without extra terms [17]. Setting

$$\cos\varphi_d = u \qquad \cos\varphi = v \Rightarrow (-\sin\varphi)\,\mathrm{d}\varphi = \mathrm{d}v \tag{B16}$$

the integral becomes [18]

$$I_{C_3} = \oint_{-1}^{+1} \frac{\sqrt{1-v^2}}{(v-u)^2}\,\mathrm{d}v = -\pi \tag{B17}$$

Using Eq. (B13) it can be inferred that

$$I_C = -\frac{2k\sin\varphi_d}{\pi} I_{C_3} = -\frac{2k\sin\varphi_d}{\pi}(-\pi) = 2k\sin\varphi_d = -2k\sin(\pi t) \tag{B18}$$

References

[1] Prandtl, L., and Tietjens, O. G., *Applied Hydro and Aeromechanics*, Dover, New York, pp. 203–222.

[2] Munk, M., "Isoperimetric Problems from the Theory of Flight," Inaugural Dissertation, Gottingen, Germany, 1919 (in German).

[3] Kroo, I., "Drag Due to Lift: Concepts for Prediction and Reduction," *Annual Review of Fluid Mechanics*, Vol. 33, 2001, pp. 587–617.

[4] Mortara, K., Straussfogel, D. M., and Maughmer, M. D., "Analysis and Design of Planar and Non-planar Wings for Induced Drag Minimization," NASA CR-189509, Annual Progress Report, 1991.

[5] Smith, S. C., "A Computational and Experimental Study of Nonlinear Aspects of Induced Drag," NASA, Technical Paper 3598, Feb. 1996.

[6] Demasi, L., "Induced Drag Minimization: A Variational Approach Using the Acceleration Potential," *Journal of Aircraft*, Vol. 43, No. 3, 2006, pp. 669–680.

[7] Ashenberg, J., and Weihs, D., "Minimum Induced Drag of Wings with Curved Planform," *Journal of Aircraft*, Vol. 21, No. 1, 1984, pp. 89–91.

[8] Frediani, A., Montanari, G., and Pappalardo, M., "Sul problema di Prandtl della Minima Resistenza Indotta di un Sistema Portante," *Proceedings of the 15th National Italian Conference AIDAA*, Nov. 1999.

[9] Smith, S. C., "A Computational and Experimental Study of Nonlinear Aspects of Induced Drag," Ph.D. Dissertation, Dept. of Aeronautics and Astronautics, Stanford Univ., Stanford, CA., June 1995.

[10] Kroo, I., and Smith, S. C., "Computation of Induced Drag with Nonplanar and Deformed Wakes," Society of Automotive Engineering Paper 901933, Sept. 1990.

[11] Prandtl, L., "Beitrag zur Theorie der tragenden Fläche," *Zeitschrift für angewandte Mathematik und Mechanik*, Vol. 16, No. 6, 1936, pp. 360–361.
[12] Bacciotti, A., *Teoria Matematica dei Controlli*, CELID, Turin, Italy, 1998, Chaps. 9–12.
[13] Reddy, J. N., *Energy and Variational Methods in Applied Mechanics*, Wiley, New York, 1984.
[14] Demasi, L., "Aerodynamic Analysis of Non-conventional Wing Confingurations for Aeroelastic Applications," Ph.D. Dissertation, Dipartimento di Ingegneria Aeronautica e Spaziale, Turin, Italy, March 2004.
[15] Hadamard, J., *Lectures on Cauchy's Problem in Linear Partial Differential Equations*, Yale Univ. Press, New Haven, CT, 1952.
[16] Mangler, K. W., "Improper Integrals in Theoretical Aerodynamics," Royal Aircraft Establishment, Report No. 2424, Farnborough, U.K., 1951.
[17] Monegato, G., "Numerical Evaluation of Hypersingular Integrals," *Journal of Computational and Applied Mathematics*, Vol. 50, Nos. 1–3, 1994, pp. 9–31.
[18] Kaya, A. C., and Erdogan, F., "On the Solution of Integral Equations with Strongly Singular Kernels," NASA CR-178138, June 1986.
[19] Cone, C., "Theory of Induced Lift and Minimum Induced Drag of Nonplanar Lifting Systems," NASA TR R-139, Jan. 1962.
[20] Munk, M., "The Minimum Induced Drag in Airfoils," NACA Report 121, 1921.
[21] Demasi, L., Chiocchia, G., and Carrera, E., "Aerodinamica dei Sistemi Portanti Chiusi: Ala Anulare Ellittica," *Proceedings of the 17th National Italian Conference AIDAA*, Sept. 2003.